

FOR REFERENCE

NOT TO BE TAKEN FROM THIS ROOM

DETERMINATION OF THERMOPHYSICAL
PROPERTIES OF POLYMER-SOLVENT PAIRS
BY GAS CHROMATOGRAPHY

BY

MUALLA ÖNER

Bogazici University Library



14

39001100314676

B.S. in Chemical Engineering
Istanbul Technical University
Faculty of chemical

1982

Submitted to the Institute for Graduate Studies in
Science and Engineering in partial fulfillment of
the requirements for the degree of

Master of Science

in

Chemical Engineering

BOĞAZIÇI UNIVERSITY

1985

ACKNOWLEDGEMENTS

I would like to express my appreciation to my thesis supervisor Prof. Dr. Salih Dinçer for his encouraging guidance, advice and invaluable supervision throughout this study.

I also want to express my thanks to Doç.Dr. Fahir Borak, the Chairman of the Chemical Engineering Department for the department's financial aid and all the other members of the Chemical Engineering Department of Boğaziçi University.

I would like to extend my thanks to Prof. Dr. Bahattin Baysal of I.T.U. and to Dr. Tunç Savaşçı of Petkim-Petrokimya A.Ş. for their help and guidance.

I am also grateful to my family and to my husband Gürses Öner for his help, patience and encouragement during this work.

ABSTRACT

In this study, thermophysical properties like Flory-Huggins interaction parameter (χ), weight fraction infinite dilution activity coefficient (Ω_1^∞), heat of solution (ΔH_s) and diffusion coefficient (D_1) were determined for polyisobutylene (PIB), antishock polystyrene and styrene-butadiene rubber (SBR) with benzene, cyclohexane, n-hexane and n-pentane using gas chromatography (GC). The experiments were performed for antishock polystyrene at 313.3 to 402.3 K, for SBR at 343.3 to 363.2 K and for PIB at two different temperatures 312.1 K and 323.1 K. The chromatographic retention data obtained at these temperatures were used to determine the above mentioned thermophysical properties of polymer-solvent pairs.

POLİMER-ÇÖZÜCÜ ÇİFTLERİNİN TERMOFİZİKSEL ÖZELLİKLERİNİN

GAZ KROMATOĞRAFİSİYLE HESAPLANMASI

ÖZET

Bu çalışmada, poliizobutilen (PIB), stiren-butadien kauçuğu (SBR) ve antişok polistiren'in, Flory-Huggins parametresi (χ), ağırlık kesirli sonsuz seyreltme aktivite katsayısı (Ω_1^∞), çözünme ısısı (ΔH_S) ve diffüzyon katsayısı (D_1) gibi termofiziksel özellikleri benzen, siklohekzan, n-hekzan ve n-pentan kullanılarak gaz kromatografisi yöntemi ile saptanmıştır. Deneyler antişok polistiren için 313.3 K'den 402.3 K'e, SBR için 343.3 K'den 363.2 K'e ve PIB için iki değişik sıcaklık, 313.1 K ve 323.1 K kullanılarak gerçekleştirilmiştir. Bu sıcaklarda alınan kromatografik alıkonma verileri, polimer-çözücü çiftlerinin yukarıda bahsedilen termofiziksel özelliklerinin saptanmasında kullanılmıştır.

TABLES OF CONTENTS

	Page
ACKNOWLEDGEMENTS	iii
ABSTRACT	iv
ÖZET	v
TABLE OF CONTENTS	vi
LIST OF TABLES	viii
LIST OF FIGURES	x
LIST OF SYMBOLS	xi
1. INTRODUCTION	1
2. INVERSE GAS CHROMATOGRAPHY	3
2.1 Retention Time	3
2.2 Retention Volume	5
3. THERMOPHYSICAL PROPERTIES OF POLYMERS BY INVERSE GAS CHROMATOGRAPHY	9
3.1 Infinite Dilution Activity Coefficient	9
3.2 Flory-Huggins Interaction Parameter	11
3.3 Glass Transition and Melting Behaviour	13
3.4 Heats of Solution	15
3.5 Diffusion Coefficients	15
4. EXPERIMENTAL SECTION	18
4.1 Apparatus	18
4.2 Materials Used in Experiments	18
4.2.1 Polyisobutylene (PIB)	18
4.2.2 Antishock Polystyrene	18

4.2.3 Styrene-Butadiene Rubber (SBR)	20
4.2.4 Support	20
4.2.5 Solvents	20
4.3 Column Preparation	20
4.4 Carrier gas Flow Rate	24
4.5 Injection Technique	24
5. RESULTS AND DISCUSSION	25
6. CONCLUSIONS AND RECOMMENDATIONS	42
6.1 Conclusions	42
6.2 Recommendations	43
LITERATURE CITED	44
APPENDICES	46
APPENDIX 1. PRODUCTION AND USES OF POLYMERS USED IN THIS STUDY	47
A.1.1 Styrene-Butadiene Rubbers	47
A.1.2 Polvisobutylene	48
A.1.3 Antishock Polystyrene	48
APPENDIX 2. NUMBER AVERAGE MOLECULAR WEIGHT DETERMINATION BY MEMBRANE OSMOMETER	49
A.2.1 Membrane Osmometer	49
A.2.2 Operation of the Osmometer	49
APPENDIX 3. RAW EXPERIMENTAL DATA	51
APPENDIX 4. REQUIRED PHYSICAL PROPERTIES OF SOLVENTS	81
A.4.1 Calculation of Saturated Vapor Pressures of Pure Solvents (P_1^S)	81
A.4.2 Estimation of Molar Liquid Volume of Solvents (V_1) ...	81
A.4.3 Second Virial Coefficient(B_{11})	81
APPENDIX 5. SAMPLE CALCULATIONS	82

LIST OF TABLES

Table 4.1	Column Characteristics	23
Table 5.1	Comparison of χ^M Values of PIB with those in Literature .	27
Table 5.2	V_g^0 , Ω_1^∞ , χ Values of Solvents with SBR at Various Temperatures	28
Table 5.3	V_g^0 , Ω_1^∞ , $\bar{\chi}$ Values of n-Hexane-Antishock Polystyrene at Various Temperatures	29
Table 5.4	V_g^0 , Ω_1^∞ , χ Values of Solvents with Antishock Polystyrene at Various Temperatures	30
Table 5.5	Diffusion Coefficients of Solvents with SBR at Variuos Temperatures	35
Table 5.6	Diffusion Coefficients of Solvents with Antishock Polystyrene at Various Temperatures	36
Table 5.7	Diffusion Coefficients of Solvents with PIB at 313.1 K .	36
Table 5.8	Heats of Solution ($-\Delta H_s$ Kcal/mole) of Various solvents with Antishock Polystyrene and SBR	39
Table A.3.1	Data for PIB-n-Pentane system at 313.1 K	52
Table A.3.2	Data for PIB-Benzene system at 313.1 K	53
Table A.3.3	Data for PIB-Cyclohexane system at 316.3 K	53
Table A.3.4	Data for SBR-n-Hexane system at 343.3 K	54
Table A.3.5	Data for SBR-n-Hexane system at 353.1 K	55
Table A.3.6	Data for SBR-n-Hexane system at 363.1 K	56
Table A.3.7	Data for SBR-Cyclohexane system at 343.3 K	57
Table A.3.8	Data for SBR-Cyclohexane system at 353.1 K	58
Table A.3.9	Data for SBR-Cyclohexane system at 363.1 K	59
Table A.3.10	Data for SBR-Benzene system at 343.3 K	60
Table A.3.11	Data for SBR-Benzene system at 353.1 K	61
Table A.3.12	Data for SBR-Benzene system at 363.1 K	62

Table A.3.13	Data for Antishock Polystyrene-Benzene system at 382.3 K	63
Table A.3.14	Data for Antishock Polystyrene-Benzene system at 394.1 K	64
Table A.3.15	Data for Antishock Polystyrene-Benzene system at 402.3 K	65
Table A.3.16	Data for Antishock Polystyrene-Cyclohexane system at 382.3 K	66
Table A.3.17	Data for Antishock Polystyrene-Cyclohexane system at 394.1 K	67
Table A.3.18	Data for Antishock Polystyrene-Cyclohexane system at 402.3 K	68
Table A.3.19	Data for Antishock Polystyrene-n-Hexane system at 382.3K	69
Table A.3.20	Data for Antishock Polystyrene-n-Hexane system at 394.1K	70
Table A.3.21	Data for Antishock Polystyrene-n-Hexane system at 402.3K	71
Table A.3.22	Data obtained for Antishock Polystyrene-n-Hexane system at various temperatures	72
Table A.3.23	Data obtained for SBR-Benzene system at various temperatures	75
Table A.3.24	Data obtained for SBR-Cyclohexane system at various temperatures	76
Table A.3.25	Data obtained for SBR-n-Hexane system at various temperatures	77
Table A.3.26	Data obtained for PIB-Benzene system at various temperatures	78
Table A.3.27	Data obtained for PIB-Cyclohexane system at various temperatures	79
Table A.3.28	Data obtained for PIB-n-Pentane system at various temperatures	80

LIST OF FIGURES

Figure 2.1	Chromatogram of a single solute	4
Figure 3.1	Generalized retention diagram for semicrystalline polymer	14
Figure 4.1	Gas Chromatographic Apparatus	19
Figure 4.2	Infrared Spectrum for Antishock Polystyrene	21
Figure 4.3	Infrared Spectrum for SBR	22
Figure 5.1	Plots of χ against temperature for solvent-antishock polystyrene binary systems	31
Figure 5.2	Glass Transition Curve of Antishock Polystyrene using n-Hexane	33
Figure 5.3	Van Deemter curves for SBR-solvent systems	37
Figure 5.4	Van Deemter curves for SBR-solvent systems at 363.1 K....	38
Figure 5.5	Effect of Gas Flow Rate on Retention Data for the column packed with Antishock Polystyrene	41

LIST OF SYMBOLS

- A : An arbitrary constant in Eq.(3.18)
 \bar{a} : Volume of gas per unit length of the column
 a_1 : Activity coefficient of solvent
 a : An arbitrary integration constant in Eq.(2.16)
 B : An arbitrary constant in Eq.(3.18) describing diffusional spreading of the vapor
 B_{11} : Second virial coefficient
 C : Slope of the Van Deemter curve
 c : Concentration of solvent
 D_1 : Diffusion coefficient of the vapor in the stationary phase
 D_g : Diffusion coefficient of the vapor in the gas phase
 d_f : Thickness of the stationary phase
 f : Fugacity
 f_p : Pressure correction factor
 H : Height equivalent to the theoretical plate in GLC
 K : Column Permeability
 K_o, K_a : Partition coefficient for surface adsorption
 K_b : Partition coefficient for bulk sorption
 K', K'' : Arbitrary constants in Eq.(2.10)
 k : Partition coefficient in Eq.(3.21)
 L, l : Column length
 M_i : Molecular weight
 \bar{M}_n : Number average molecular weight of the polymer
 m_2 : Polymer amount in the column
 n_i : Mole number

- P : System Pressure
 P_i : Pressure at the inlet of the column
 P_o : Pressure at the outlet of the column
 P_1^s : Saturated vapor pressure of solvent
 p : Partial Pressure
 Q : Carrier gas flow rate at room temperature and atmospheric pressure
 R : Gas constant
 T : System temperature
 T_g : Glass transition temperature
 T_m : Melting point temperature
 T_{r_m} : Room temperature
 t_A : Retention time of reference gas (air)
 t_R : Retention time of injection solvent
 t_R' : Adjusted retention time of solute in Eq.(2.1)
 u : Linear carrier gas velocity
 V_g^o : Specific retention volume corrected to 0°C and 1 atm
 V_M^o : The corrected gas hold-up volume
 V_N^o : Net retention volume
 V_R : Measured retention volume
 V_R^o : Retention volume corrected for pressure
 \dot{V} : Volumetric flow rate of carrier gas at any condition
 V_i : Molar volume
 $\dot{V}_{o,Q}$: Volumetric flowrate measured at the outlet of column
 V_{2sp} : Specific volume of polymer
 V^* : Specific core volume
 $w_{1/2}$: Measured peak width at half height
 w_1 : Weight fraction of the solvent

- X : Direction along the column
- x_i : Mole fraction in liquid phase
- β : An arbitrary integration constant in Eq.(2.16)
- ζ : Constant in Eq.(3.19)
- γ : Mole fraction activity coefficient
- ΔG_M : Gibbs Free Energy of mixing
- ΔH_S : Heat of solution
- δ : Coverage ratio
- μ_1 : Chemical potential
- η : Gas viscosity
- ρ : Density
- ν : A parameter in Eq.(5.1)
- Π : Osmotic pressure
- ϕ : Volume fraction
- τ : A parameter in Eq.(5.1)
- χ : Flory-Huggins Parameter
- χ^* : Specific interaction parameter based on hard core volume
- Ω_1^∞ : Weight fraction infinite dilution activity coefficient

Subscripts

- a : Adsorption
- B : Spherical beads
- b : Bulk sorption
- g : Gas phase
- 1,i: Inlet
- N : Net
- n : Number Average
- o : Outlet
- R : Retention
- r : Reference gas or room conditions
- p : Polymer
- s : solution
- sp : Specific
- 1 : Solvent
- 2 : Polymer

Superscripts

- M : Mixing
- s : Saturated property
- V : Vaporization
- o : Standard state
- ∞ : Infinite dilution

I. INTRODUCTION

Gas chromatography has been recently replacing the static methods for measuring the thermophysical properties of various systems, especially polymer-solvent systems. This technique is preferred to static techniques because it is simple, economical, practical and requires very small amounts of polymer and solvent (1,2,3,4,5).

The main purpose of this study was to obtain certain thermophysical parameters and solution properties of industrially important polymers, polyisobutylene (PIB), antishock polystyrene and styrene-butadiene rubber (SBR) with four different solvents by using inverse gas chromatography. The thermophysical parameters in consideration, here, are weight fraction infinite dilution activity coefficient, Flory-Huggins interaction parameter, heat of solution and diffusion coefficient at various temperatures. These parameters are especially useful for solvent selection and equipment design in the polymer processing industry, e.g. for separators, dryers and chemical reactors.

The solvent volatility at large polymer concentrations is related to the infinite dilution activity coefficient (4). Especially for the understanding of the drying of polymer coating films, it is necessary to know the volatility of the solvent over the coating film at small solvent concentrations. This parameter is also related to the solubility. In order to achieve good solubility, infinite dilution activity coefficient should have a very small value. It also provides a convenient measure for comparing polymer-solvent interactions for a series of solvents with a given polymer.

The thermodynamic properties of polymer solutions are frequently described in terms of Flory-Huggins interaction parameter (χ) which is a measure of the strength of interaction between polymer and solvent. This parameter comes from differences in intermolecular forces between solvent and polymer. A negative or low positive value of χ indicates a

favorable tendency to form a solution, whereas a high value of χ indicates that the polymer is insoluble in the solvent. According to Flory-Huggins theory for complete miscibility of a polymer and solvent, the value of χ should be less than or equal to 0.5 (6).

The application of GLC for the determination of glass transition and melting transition curve is also a recent technique (7). As the temperature of a polymer melt or rubber is lowered, a point known as the glass-transition temperature (T_g) is reached where polymeric materials undergo a marked change in properties associated with the virtual cessation of molecular motion on the local scale. Below their glass transition temperature, polymers have many of the properties associated with ordinary inorganic glasses including hardness, stiffness, brittleness and transparency. T_g can be determined by differential thermal analysis, too. The gas chromatographic determination yields a curve describing the glass transition and melting behaviour depending on the adsorption and desorption mechanism of solvent vapor on the surface of polymeric material.

From the shape of the eluting solvent peak, information can also be gained on the kinetic processes operative in a GC column. As the solvent progresses from inlet to outlet, the band of solvent molecules broadens due to diffusional spreading in both gas and liquid phases. Under suitable experimental conditions the diffusion coefficient of the solvent in the polymer stationary phase can be determined from the width of symmetrical eluted peak (8).

The observations performed by using inverse GLC, as in this study, aims to present thermophysical data for polymer-solvent pairs. The effects of various chromatographic conditions and carrier gas flow rates on retention data and on the thermophysical properties, are also instructive for further study on this subject.

2. INVERSE GAS CHROMATOGRAPHY

In principle, the most satisfactory method of studying polymers by GLC involves the use of "Inverse Chromatography" (7). Whereas in conventional GLC property of an "unknown" sample in the moving phase is determined by its interaction with a "known" stationary phase, in inverse chromatography, the properties of an "unknown" stationary phase are investigated by their interactions with a specific moving phase (probe solutes, or molecular probe). The vaporizable molecules in the gas phase are designated as "probe" molecules by Guillet (9) who refers to this experiment as a "molecular probe" experiment.

2.1 Retention Time

After the solvent is injected into the column, the time required to sweep the solvent in the carrier gas from the column, is called the retention time. Figure 2.1 illustrates the chromatogram of a single solvent (10). A sample consisting of the solvent and some inert gas (air) enters the column at time = 0, the starting point of the chromatogram. The inert gas does not interact with the stationary phase and emerges at point A with the carrier gas, which enters the column with the sample. Consequently, time t_A measured from the starting point 0 to the inert gas peak maximum. OA is equal to the time needed by the carrier gas to move from one end of the column to the other and is called retention time of an unadsorbed gas. Since air is used most conveniently for the determination of t_A , the inert gas peak is often called the air peak and t_A is described as the air peak time.

Retention time of the solvent, t_R , is the time that elapses between the injection of the sample and recording of the peak maximum. It is equal to the distance OB in Fig.2.1.

Adjusted retention time of the solvent, t'_R , is the time that elapses between the emergence of the inert gas and the solvent peak maxima. It is

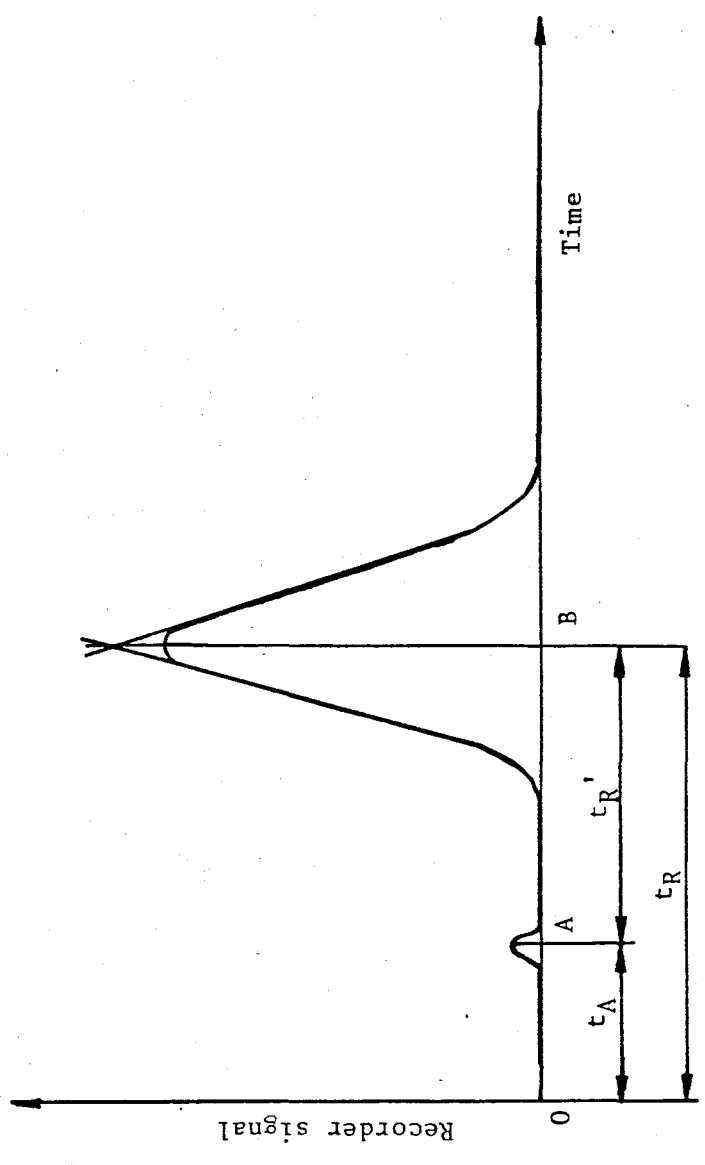


Fig. 2.1.1. Chromatogram of a single solvent

equal to the distance AB. Thus

$$t'_R = t_R - t_A \quad (2.1)$$

$$t_R = t_A + t'_R \quad (2.2)$$

Eq.(2.2) expresses the fact that the retention time of solvent is the sum of the time spent by the solvent in the gas phase, t_A , and the time during which the solvent is sorbed by the stationary phase, t'_R . Hence, t_A is often described as the gas hold-up time and t'_R as the liquid hold-up time when liquid stationary phase is used.

2.2 Retention Volume

The volume of carrier gas which flows through the column during the retention time is described as the retention volume. The employment of corrected retention volumes is necessary when gas chromatographic data are related to the thermophysical properties.

Retention volumes are calculated from the corresponding retention times and from the flow rate of the carrier gas. Due to the pressure drop across the column and the compressibility of the carrier gas, the actual flow rate varies from point to point in the column. The true retention volume can be obtained by multiplying with a pressure correction factor. The general relation between retention time and volume is written as (11):

$$t_R = \int_0^{V_R^0} \frac{dV}{\dot{V}} \quad (2.3)$$

where \dot{V} is the volumetric flowrate of carrier gas. Boyle's law can be stated as :

$$P_0 \dot{V}_0 = P \dot{V} \quad (2.4)$$

where P_0 and \dot{V}_0 are the pressure and the volumetric flowrate measured at the outlet of the column. If we solve for \dot{V} from Eq.(2.4) and substitute into Eq.(2.3) we obtain :

$$t_R = \int_0^{V_R^0} \frac{P dV}{\dot{V}_0 P_0} \quad (2.5)$$

Hence \dot{V} is a function of X , the distance from inlet end of the column. The variable of integration can be changed as :

$$V = X (a + m\beta) \quad (2.6)$$

where a , β and m are chromatographic characteristics (11). Then Eq.(2.5) is written as :

$$t_R = (a + m\beta) \int_0^L \frac{P dX}{\dot{V}_0 P_0} \quad (2.7)$$

where L is the length of the column.

The relation between the pressure gradient $\frac{dP}{dX}$ and the volumetric flow rate \dot{V} is (11) :

$$\frac{dP}{dX} = - \frac{\eta}{K} \dot{V} \quad (2.8)$$

where η is the gas viscosity and K is the "Column Permeability" parameter. By substituting Eq.(2.4) into Eq.(2.8) we obtain :

$$\frac{dP}{dX} = - \left[\eta \frac{P_0 \dot{V}_0}{K} \right] \frac{1}{P} \quad (2.9)$$

The solution of this equation is simplified by the fact that the gas viscosity is independent of pressure, so that all the quantities in the square bracket can be regarded as constant denoted by $-K'$. Solving Eq. (2.9) gives :

$$X = \frac{P^2}{2K'} + K'' \quad (2.10)$$

where K'' is another constant. The boundary conditions are :

$$P = P_i \quad , \quad \text{when } X = 0 \quad (2.11)$$

$$P = P_o \quad , \quad \text{when } X = L \quad (2.12)$$

where subscripts i , o denote inlete and outlet conditions. Using Eqs. (2.11) and (2.12) in Eq.(2.10) gives :

$$K' = \frac{P_o^2 - P_i^2}{2L_i} \quad , \quad K'' = - \frac{P_i^2}{2K'} \quad (2.13)$$

In this study, P_o , is taken as atmospheric pressure. Combining Eqs.(2.7), (2.9), (2.10) gives :

$$t_R = (a + m\beta) \int_{P_i}^{P_o} \frac{P^2 dP}{K' \dot{V}_o P_o} \quad (2.14)$$

Substituting K' into Eq. (2.14) and integrating yields :

$$t_R \dot{V}_o = L (a + m\beta) \left[\frac{2}{3} \cdot \frac{(P_i/P_o)^3 - 1}{(P_i/P_o)^2 - 1} \right] \quad (2.15)$$

In this equation, the left hand side, i.e., the product of the outlet flow rate and the measured retention time, is the measured retention volume (V_R). The first term on the right hand side of Eq. (2.15) is defined as the true retention volume (V_R^o) :

$$V_R^o = L (a + m\beta) \quad (2.16)$$

Thus, the expression in Eq. (2.15) in square brackets is the correction factor required to correct the measured retention volume for the effect of the pressure drop across the column. The equation can be rewritten as (11) :

$$V_R^o = V_R \times \left[\frac{3}{2} \cdot \frac{(P_i/P_o)^2 - 1}{(P_i/P_o)^3 - 1} \right] = f_p V_R \quad (2.17)$$

where f_p is the pressure correction factor and is defined as :

$$f_p = \frac{3}{2} \cdot \frac{(P_i/P_o)^2 - 1}{(P_i/P_o)^3 - 1} \quad (2.18)$$

The correct gas hold-up volume of the column V_M^o can be calculated by similar equations :

$$V_M^o = V_M f_p = t_A \dot{V}_o f_p \quad (2.19)$$

In measuring the carrier gas volume velocity \dot{V}_O , one must take into consideration the temperature correction factor $(273.2/T_{r_m})$ where T_{r_m} is room temperature and the polymer amount (m) in the column. Thus, the specific retention volume corrected to 0°C can be obtained as the volume per unit weight of the polymer, from the following expression :

$$V_g^o = V_R^o - V_M^o = \dot{V}_O (t_R - t_A) \left(\frac{273.2}{T_{r_m}} \right) \left(\frac{f}{m} \right) \quad (2.20)$$

3. THERMOPHYSICAL PROPERTIES OF POLYMERS BY GAS CHROMATOGRAPHY

3.1 Infinite Dilution Activity Coefficient

The distribution of the solvent between the stationary and mobile phase is expressed by the dimensionless partition coefficient, K_0 . It is defined as :

$$K_0 = \frac{\text{amount of solvent in the stationary phase}}{\text{amount of solvent in the mobile phase}}$$

K_0 is simply determined from GLC through

$$K_0 = V_N^0 / V_1 \quad (3.1)$$

where V_N^0 is net retention volume and V_1 is volume of liquid phase in column. At an early point in the development of glc, it seemed advisable to convert K_0 to a quantity considered characteristic of the interaction between the two components in the liquid phase. It is reported that (12) the chosen quantity has been rational activity coefficient, γ_1 , of component 1. This is defined as the ratio of the activity (a_1) i.e., the ratio of the fugacity f_1 to the fugacity f_1^0 in the standard state of pure liquid 1, to the mole fraction, x_1 . Thus :

$$\gamma_1 = \frac{a_1}{x_1} = \frac{f_1}{x_1 f_1^0} \quad (3.2)$$

If the gas is ideal i.e., $f_1 = P_1$, and $f_1^0 = P_1^S$, Eq. (3.2) gives for γ_1 $x_1 \rightarrow 0$:

$$\gamma_1^\infty = RTN_{2,liq} / P_1^S V_N^0 \quad (3.3)$$

where $N_{2,liq}$ is the number of moles of component 2 in the liquid phase. Correcting for the effect of finite pressure, P_1^S , on the chemical potential of component 1 in gas and liquid states, Eq. (3.3) becomes :

$$\ln \gamma_1^\infty = \ln \left(\frac{RTN_{2,liq}}{P_1^S V_N^O} \right) - \frac{P_1^S}{RT} (B_{11} - V_1) \quad (3.4)$$

where B_{11} is the gas-state second virial coefficient of component 1, V_N^O is the net retention volume and V_1 molar volume of the pure solvent. Converting net retention volume V_N^O to V_g^O , which is expressed per gram of liquid phase and corrected to 0°C using the ideal gas relation, Eq. (3.4) can be written as :

$$\ln \gamma_1^\infty = \ln \left(\frac{273.2 R}{P_1^S V_g^O M_2} \right) - \frac{P_1^S}{RT} (B_{11} - V_1) \quad (3.5)$$

where M_2 is the molecular weight of liquid phase. However, it was pointed out that (7) the method becomes inaccurate for molecular weights exceeding about 1500. Since most high polymers have molecular weights exceeding about 10000, the inclusion of the M_2 term in Eq. (3.5) presents a serious difficulty. Therefore, it is more useful to consider the ratio of the activity a_1 to a weight fraction of the polymeric component. If we choose weight fraction, Eq. (2.5) becomes :

$$\ln \left(\frac{a_1}{w_1} \right)^\infty = \ln \Omega_1^\infty = \ln \left(\frac{273.2 R}{P_1^S V_g^O M_1} \right) - \frac{P_1^S}{RT} (B_{11} - V_1) \quad (3.6)$$

where the denominator now contains M_1 , the molecular weight of the probe, not of the polymer molecule. This important relation permits the experimental determination of thermodynamic properties of polymer solutions at infinite dilution of the solvent in the polymer phase.

3.2 Flory-Huggins Interaction Parameter

The gas-liquid chromatographic experiments can be useful in providing a rapid, readily applicable route to the evaluation of thermodynamics of polymer solutions. The technique can be particularly valuable for the determination of χ parameter which is a measure of the strength of interaction between polymer and solvent.

For a binary system (polymer-solvent pair), the volume fraction is given by :

$$\phi_1 = \frac{x_1 V_1}{x_1 V_1 + x_2 V_2} \quad (3.7)$$

and

$$\phi_2 = 1 - \phi_1 \quad (3.8)$$

where x is the mole fraction, V_1 and V_2 are the molar volumes of the low molecular weight substance and the polymer, respectively.

According to Flory-Huggins theory, Gibbs free energy of mixing for a polymer-solvent pair is given as (6,13) :

$$\Delta G_M = RT \chi n_1 \phi_2 + RT (n_1 \ln \phi_1 + n_2 \ln \phi_2) \quad (3.9)$$

where χ is a dimensionless quantity which characterizes the interaction energy for a polymer-solvent pair.

If the above equation is differentiated with respect to n_1 holding χ parameter constant, the chemical potential μ_1 of the solvent in the solution relative to its chemical potential μ_1^0 in the pure liquid is obtained :

$$\frac{\mu_1 - \mu_1^0}{RT} = \left[\ln \phi_1 + \left(1 - \frac{V_1}{V_2}\right) \phi_2 \right] + \chi \phi_2^2 \quad (3.10)$$

Using the following expression for the activity a_1 of the solvent :

$$\ln a_1 = \frac{\mu_1 - \mu_1^0}{R T} \quad (3.11)$$

and by substituting Eq. (3.10) into Eq. (3.11) we obtain :

$$\ln a_1 = \left[\ln \phi_1 + \left(1 - \frac{V_1}{V_2}\right) \phi_2 \right] + \chi \phi_2^2 \quad (3.12)$$

Theories of solution thermodynamics express the activity of a component as the sum of two contributions (i) a combinatorial (or athermal) entropy, first term in Eq. (3.12) (ii) a noncombinatorial (or thermal) contribution, second term in Eq. (3.12). The latter contribution is characteristic of the polymer-solvent pair and its determination is the goal of activity measurements in polymer solutions (14,15).

For the limiting case in which $\phi_2 \rightarrow 1$, combining Eqs. (3.5), (3.7) and (3.12) and letting (14,16) :

$$V_2 = V_{2sp} \bar{M}_n \quad (3.13)$$

Eq. (3.12) becomes :

$$\chi = \ln \left(\frac{273.2 R V_{2sp}}{V_{g1}^{OP} V_1} \right) - \left(1 - \frac{V_1}{\bar{M}_n V_{2sp}} \right) - \frac{P_1^S}{RT} (B_{11} - V_1) \quad (3.14)$$

where \bar{M}_n is the number average molecular weight of polymer, V_{2sp} is the specific volume and V_2 is the molar volume of polymer.

There is both theoretical and experimental justification, for regarding χ in Eq. (3.14) as being concentration dependent (14). In view of this, two points are stressed : (i) the value of χ at infinite dilution obtained by glc will in general differ from that obtained at other concentrations by conventional methods, and (ii) the glc value of χ in Eq. (3.14) is the whole noncombinatorial contribution to $\ln a_1$ at infinite dilution.

In literature (12), it is also advised to use the following expression :

$$\chi^* = \ln \left(\frac{273.2RV_2^*}{P_1^S V_g^O V_1^*} \right) - \left(1 - \frac{V_1^*}{M_n V_2^*} \right) - \frac{P_1^S}{RT} (B_{11} - V_1) \quad (3.15)$$

Here, χ^* is specific interaction parameter based on hard core volume. In this equation Flory replaced volume fraction in Eq. (3.14) with segment fraction and specific volumes with specific core volumes.

3.3 Glass Transition and Melting Behavior

In glc, solvent-solute interactions can be related to the specific retention volume. The generalized retention diagram of the logarithm of the specific retention volume versus reciprocal of the absolute temperature is a linear plot in the absence of any transitions. A z-shaped curve such as shown in Fig. 3.1 is indicative of a glass transition (17,18).

In the temperature region corresponding to segment AB of Fig. 3.2, the polymer is below its glass transition temperature (T_g) and penetration of the solvent molecules into the bulk of polymer phase is precluded. Retention proceeds exclusively by surface adsorption and the corresponding retention diagram is linear. Information on the surface properties of polymer can be obtained in this temperature range (7).

The deviation from linearity represented by point B can be related to the glass transition temperature of the polymer (19,20). The region BC corresponds to nonequilibrium absorption of the probe molecules in the polymer phase. As the temperature is increased in region BC the diffusion coefficient rises sharply, leading to equilibrium conditions at point C.

At temperatures below the melting point of the polymer, in region CD, equilibrium absorption of the probe molecules in the amorphous phase of the polymer occurs. Retention in the region is caused by two processes : (1) Surface adsorption, and (2) solution in the bulk polymer phase. The behaviour in this region can be formulated as (18) :

$$V_R = K_b m_1 + K_a A_1 \quad (3.16)$$

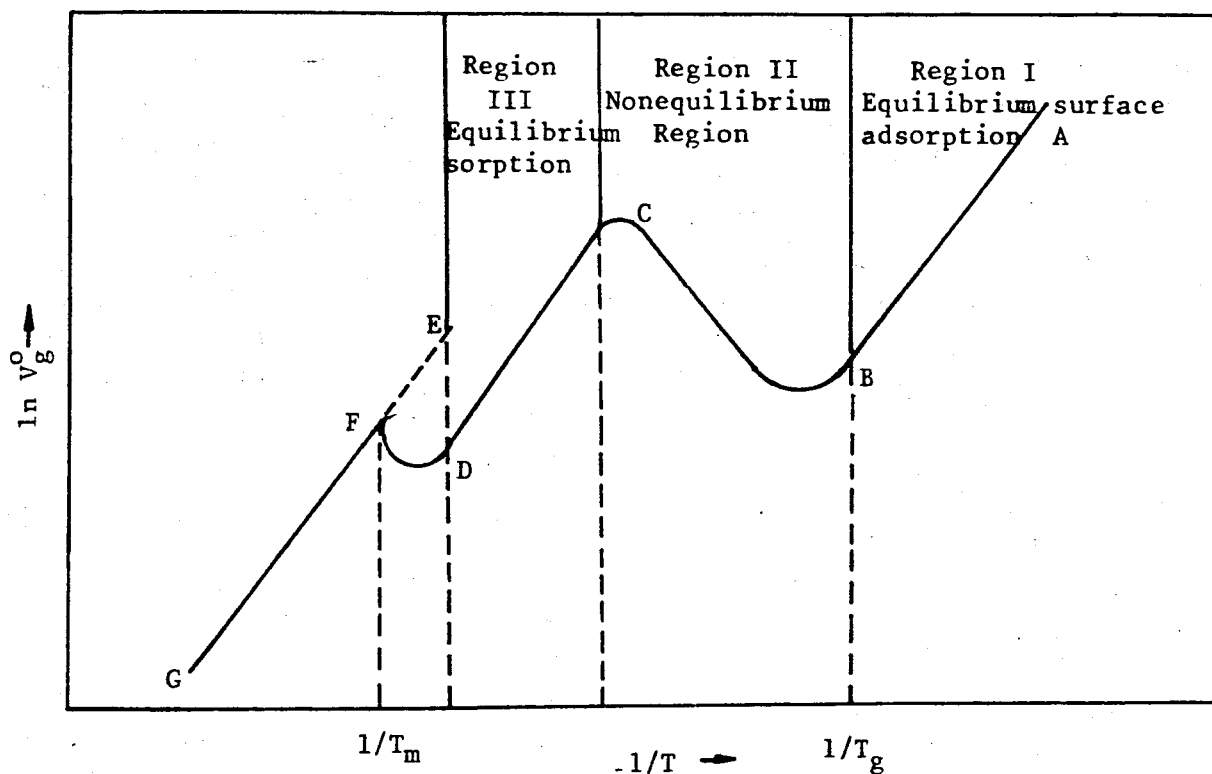


Fig. 3.1. Generalized retention diagram for semicrystalline polymer

where V_R is the retention volume, K_b and K_a are the partition coefficients for bulk sorption and surface adsorption, m_1 and A_1 are the mass and surface area of the stationary phase.

Upon melting, in region DF, the fraction of amorphous material increases, leading to an increase in retention volume. At temperatures above the melting point, segment FG, a linear retention diagram, corresponding to bulk sorption into the completely amorphous polymer is obtained. By extrapolation of this line to lower temperatures (dashed line FE), the crystalline content of the stationary phase can be determined by comparison of the experimental retention volume with the extrapolated value. In region FG the polymer is completely amorphous and the properties of the polymer-solvent solution can be investigated. For most polymers, equilibrium bulk sorption is achieved at temperatures in excess of about $T_g + 40^\circ\text{C}$ or 50°C .

3.4 Heat of Solution

The heat of solution ΔH_s is the total heat measured calorimetrically when two distinct phases (i.e., solvent and solute) are brought together and form a single phase (i.e. solution) (21). In our case, heat of solution can only be determined for equilibrium bulk sorption of retention diagram. It is only in this region that the polymer behaves truly as amorphous liquid. In this region, we determine heat of solution (ΔH_s) at infinite dilution using the approximate relation (2,22) :

$$\ln V_g^0 = - \frac{\Delta H_s}{R} \frac{1}{T} \quad (3.17)$$

The quantity ΔH_s represents the enthalpy change associated with the transfer of one mole of pure solvent vapor at one atmosphere into infinitely dilute solution in the molten polymer.

3.5 Diffusion Coefficients

The shapes of eluted peaks in gas chromatography on polymeric substrates are governed by several factors, one of the most important being slow diffusion in the polymer phase. By a suitable choice of conditions, the simple Van Deemter equation enables diffusion coefficients to be calculated from the variation in chromatographic peak width with carrier gas flow rate (8,17,23).

Van Deemter first related peak broadening and column properties through the relation :

$$H = A + \frac{B}{u} + Cu \quad (3.18)$$

where H is the height-equivalent to the theoretical plate, u is the linear velocity of carrier gas in the column, A,B,C are constants independent of flow rate (24). The constant A takes into account instrumental broadening while B describes the diffusional spreading of the vapor as it is eluted in the gas phase and can be expressed as :

$$B = 2\zeta D_g \quad (3.19)$$

where D_g is the diffusion coefficient of the vapor in the gas phase and ζ is a constant less than unity. In the simple Van-Deemter approach, we can write :

$$C = \frac{8 d_f^2}{\pi^2 D_1} \frac{k}{(1+k)^2} \quad (3.20)$$

where d_f is the thickness of the stationary phase, D_1 is the diffusion coefficient of the vapor in the stationary phase and the partition coefficient ratio k , is equal to :

$$k = \frac{t_R - t_A}{t_A} \quad (3.21)$$

where t_R is the retention time of solvent vapor, and t_A is the time for the carrier gas to pass through the column. The determination of D_1 involves the measurement of H at several velocities, u . From the resulting plot, the slope C of the linear portion obtained at high velocity ($B/u \rightarrow 0$) provided that d_f and k are known.

The plate height H was determined from the eluted peaks as displayed on a strip chart recorder by the relation (8) :

$$H = \frac{1}{5.54} \left(\frac{w_{1/2}}{t_R} \right)^2 \quad (3.22)$$

where t_R is the retention time from injection to peak maximum, $w_{1/2}$ is the measured peak width at half height, and l is the column length. The linear portion of a graph of H versus u is used to calculate C in the Van Deemter equation. The volumetric flow rate Q is converted to linear velocity u in the column by the relation :

$$u = (f_p Q / \bar{a}) (T_c / T_F) \quad (3.23)$$

where T_c and T_F are column and flowmeter temperatures respectively. \bar{a} is the volume of gas per unit length of the column, and f_p is defined by Eq. (2.18).

The value of \bar{a} for a given column may be determined by dividing the retention volume for a noninteracting substance, such as air by the column length, l .

The average thickness of the polymer layer d_f was found, using the relation (24) :

$$d_f = (\delta / \rho_p) / (3 / R\rho_B) \quad (3.24)$$

where ρ_p is the density of the polymer, δ is the coverage ratio (g polymer / g glass beads), R and ρ_B are the radius and density of the spherical bead, respectively.

4. EXPERIMENTAL SECTION

4.1. Apparatus

The gas chromatograph used was a Shimadzu Moduline GC-8APT with a thermal conductivity detector and Shimadzu R-111 recorder and Shimadzu C-R1B data processor. A schematic diagram is shown in Fig.4.1. Column oven temperature was measured within $\pm 0.1^{\circ}\text{C}$ by use of the Meter Digital Thermometer (Model D96M). The inlet pressure of the column was read by a mercury manometer with a precision of $\pm 1\text{mmHg}$ (Up to 1 atm). At high pressures, mercury manometer could not be used and the pressure was read directly on the apparatus with a precision $\pm 0.25\text{kg/cm}^2$. The ambient pressure was determined by a mercury barometer. Flow of the helium carrier gas was controlled by a Horning precision regulator valve. Carrier gas flow rates, in the range of 10-150ml/min were measured at room temperature by a soap-film flowmeter. The values of retention times were obtained by using data processor.

4.2. Materials Used in the Experiments

4.2.1. Polyisobutylene (PIB)

Polyisobutylene, obtained from U.S.A., contains about 2 % polyisoprene. The isoprene is used to provide preferred crosslinking site. Its number average molecular weight was determined as 860000 ± 2000 by membrane osmometer. Its density is 0.9 g/cm^3 .

4.2.2. Antishock Polystyrene

Antishock Polystyrene was supplied by Petkim-Petrokimya A.Ş.. Its density is 0.915 g/cm^3 . Its number average molecular weight was determined as 73000 ± 1000 by membrane osmometer. It is available in opaque, naturally white granules and usually contains about 5-10 % polybutadiene. The micro-

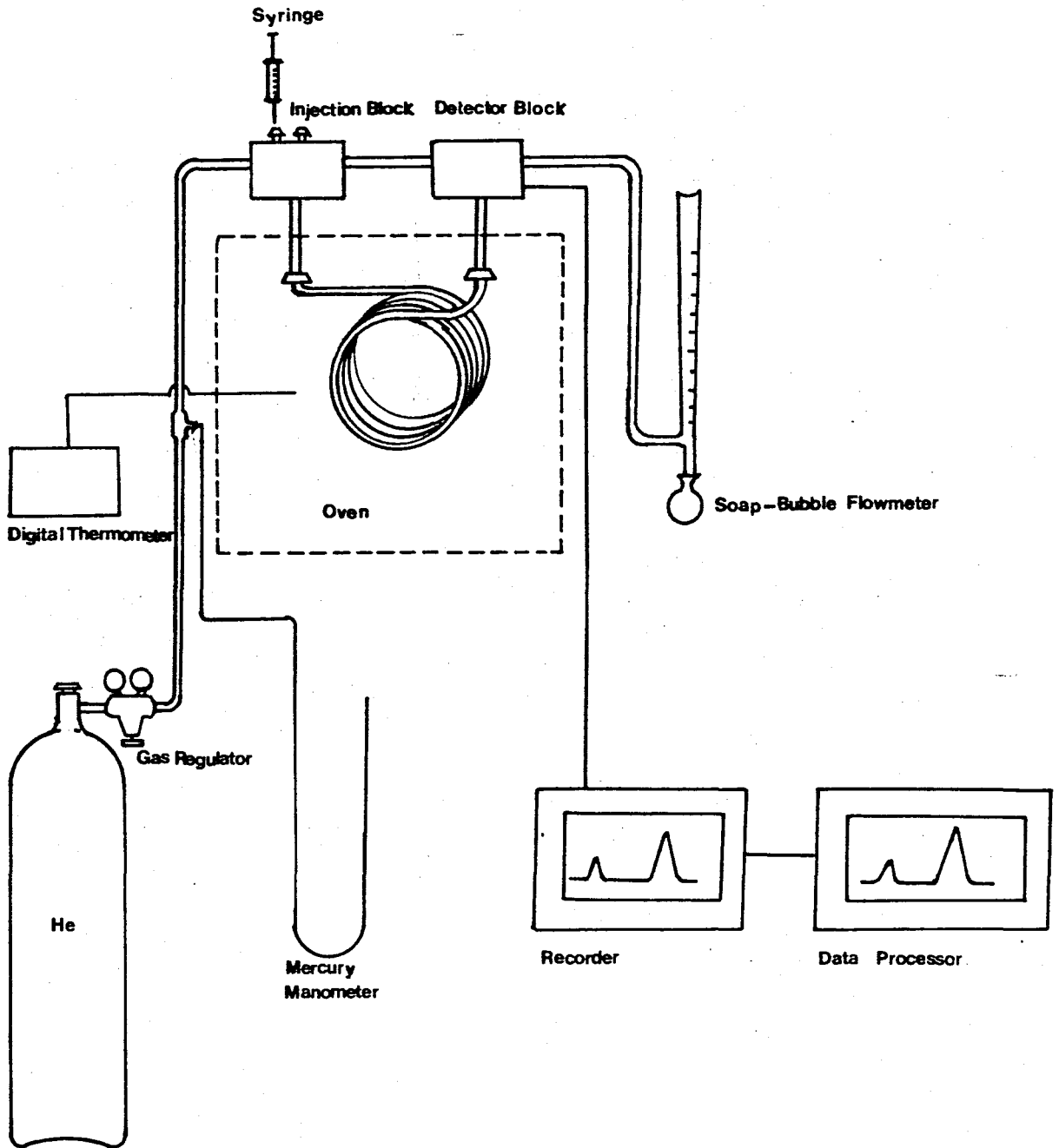


Fig. 4.1. Gas Chromatographic Apparatus

structure of the polymer is shown by infrared analysis to consist of polybutadiene (see Fig. 4.2.) (25).

4.2.3. Styrene-Butadiene Rubber (SBR).

SBR was supplied by Petkim with a product code SBR-1502 and known as cold rubber. It has a density of 0.933 g/cm^3 . Its number average molecular weight was determined as 170000 ± 3000 by membrane osmometer. It contains 20-24 % polystyrene and 70-75 % polybutadiene. The infrared analysis of the polymer is shown in Fig. 4.3 (25).

4.2.4. Support

Chromosorb P (AW-DMCS), was used as a support material in this work. Its mesh size was 80/100.

Chromosorb P is made without the use of flux. It therefore preserves a pore structure that is highly similar to that of the original diatom skeletons. This pore structure is ideal for gas chromatography. The physical properties of Chromosorb P are given as follows (26) :

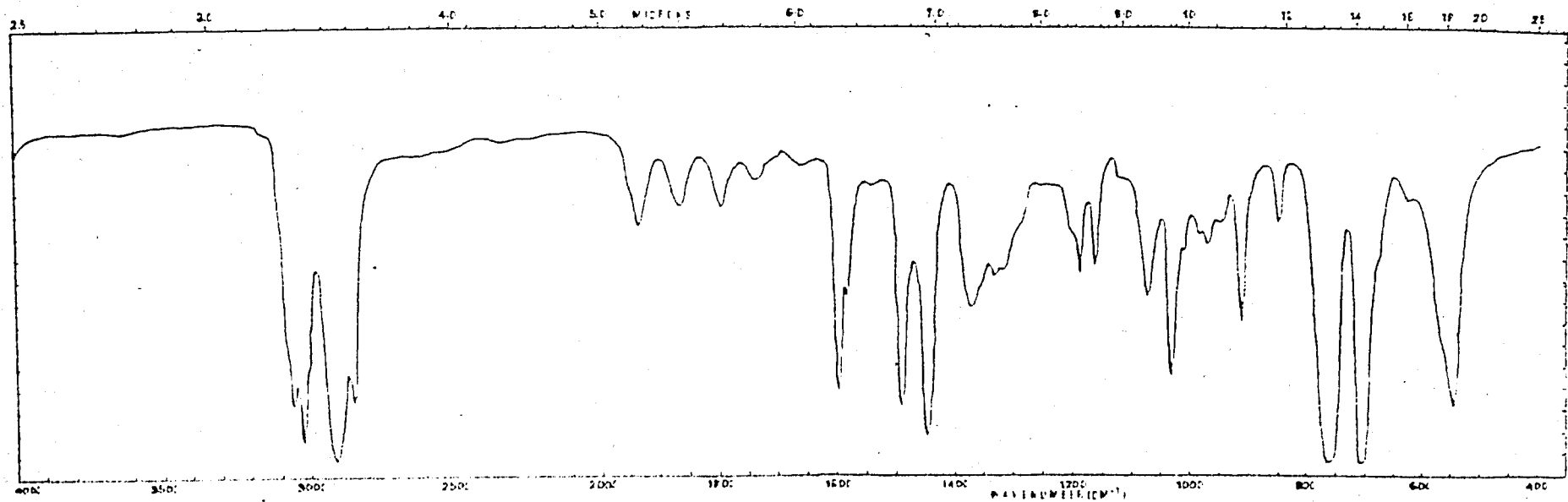
Color : Pink	Max.liquid phase loading : 30 %
Type : Calcined	pH : 6.5
Density (g/cc) : 0.47	Surface area (m^2/g) : 4

4.2.5. Solvents

Four kinds of solvents namely benzene, cyclohexane, n-hexane and n-pentane were used in experiments. All the solvents used were reagent grade materials obtained from Merck Company and they were used as received.

4.3. Preparation of Columns

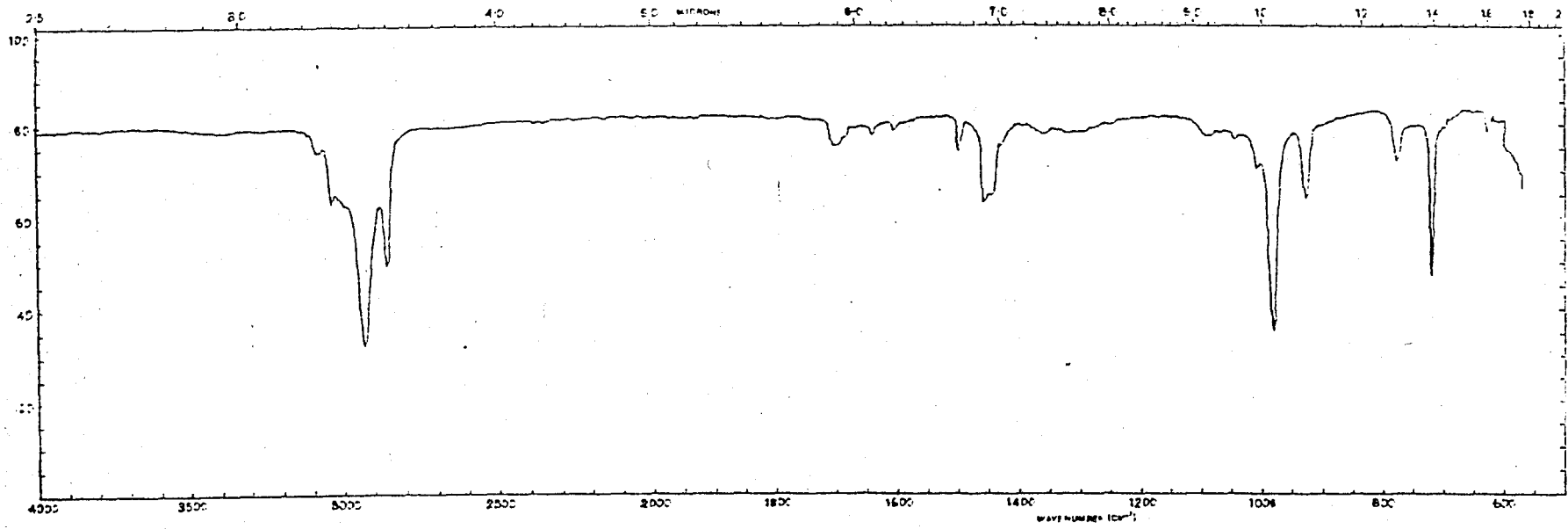
The amounts of polymers used in preparing the columns and other column characteristics are listed in Table 4.1.



Positions of characteristic infrared bonds (41,42) :

<u>Group</u>	<u>Frequency range (cm⁻¹)</u>
monosubstituted benzene	700-750 (strong)
Benzene ring	1400-1600
monosubstituted benzene	1800-2000(weak)
CH	2880-2900
= C - H	3000-3100

Fig. 4.2. Infrared Spectrum for Antishock Polystyrene (25).



Positions of characteristic infrared bonds (41,42) :

<u>Group</u>	<u>Frequency range (cm⁻¹)</u>
- CH = CH - (cis)	650-750
- CH = CH - (trans)	960-970
CH ₂	2853 ± 10 , 2926 ± 10
CH	2880-2900

Fig. 4.3. Infrared Spectrum for SBR (25).

TABLE 4.1.
 COLUMN CHARACTERISTICS
 (Column Loading 10 %)

Column	Column length (cm)	Polymer used	Polymer Amount	Support (Chromosorb P) (g)
(1) 1/8"ss	100.10	Polyisobutylene †	0.340	3.060
(2) 1/8"ss	100.00	Antishock Polystyrene ††	0.380	3.420
(3) 1/8"ss	100.00	Styrene-Butadiene Rubber ††	0.368	3.312
(4) 1/8"ss	100.10	Chromosorb P only	-	3.350

† Polyisobutylene was obtained from U.S.A.

†† SBR-1502 and Antishock Polystyrene were supplied by Petkim-Petrokimya A.Ş.

Stainless steel tubing, 1/8" o.d. and ~ 1 m length used in the experiments, were washed with hydrochloric acid (30% in water), distilled water, alcohol and acetone. Thereafter they were dried at 105°C in an oven for about six to eight hours until constant weight was attained.

The columns were prepared by first dissolving a weighed amount of polymer in benzene and then stirring the solution with a weighed amount of solid support. The whole system was heated at about 75-80°C until all of the solvent was evaporated. The particles were then dried under vacuum at 80-85°C to constant weight. The coated chromosorb was then placed into the previously prepared stainless steel tube with the aid of mechanical vibrator and vacuum pump. After the column was loaded, the two ends were plugged with glasswool in order to prevent transport of the solid particles out of the column.

The selection of support material is very important for this study because the quantitative relation between the retention volume and the

volatility of solvent in the polymer solution assumes that the peaks from the detector should be symmetric (Gaussian) in shape. The asymmetry is due to interactions between solvent and support. In this work, Chromosorb P was used because this support gives symmetric peaks with nonpolar solvents (4).

The purpose of using inert solid support was to increase available surface area of the polymer for absorption and desorption. Loadings of approximately 10 % by weight were used for all of the three kinds of polymers studied. The higher loadings usually give more pronounced deviation from normal gas-liquid chromatographic behaviour in other words a strong reversal from linear behaviour occurs. On the other hand lower loadings give nearly linear retention diagrams. Therefore, 10 % loading by weight was considered as the reasonable liquid phase loading.

For styrene-butadiene copolymers, due to three dimensional polymerizations, gel portions were observed. This impurity, which was insoluble in benzene, remained as a swollen gel. The suspension was centrifuged and then gel portion was removed. It was dried at 105°C, in an oven for about 24 hours and then weighed. In this way about 12 % by weight gel portion was found.

4.4 Carrier Gas Flow Rate

The effect of gas flowrate on specific retention volume data was observed in this study. The flow rate vs specific retention volume curves were obtained. As seen in Fig. 5.5 data were extrapolated to zero flow rates so that flow rate effect on retention data is corrected.

4.5. Injection Technique

Solvents were injected through a silicone rubber septum using a 1 µl Hamilton Syringe. The retention time at peak maximum was independent of sample size over the range 0.02-0.1 ml. Sample size of about 0.05-0.1 ml was used for all measurements which we consider to be equivalent to infinite dilution. In order to obtain air retention time about 0.1 ml of air was injected along with the liquid sample. This allowed the corrected retention time to be obtained directly from the recorder chart.

5. RESULT AND DISCUSSION

Experimental data were obtained for PIB with three solvents at two different temperatures (313.1, 323.1) to compare with data reported in literature. Data were obtained for Antishock Polystyrene at twelve different temperatures in the range of 313.3 to 402.3 K to obtain glass transition curve. Data for SBR at four different temperatures (343.3 K, 353.1 K, 358.3K, 363.2 K) were obtained. In this study the solvents benzene, cyclohexane, and n-hexane were used for Antishock Polystyrene and SBR. With PIB benzene, cyclohexane and n-pentane were used. The raw experimental gas chromatographic data are shown in Appendix I, Tables A.3.1 to A.3.28.

Retention volumes, weight fraction activity coefficients at infinite dilution and Flory-Huggins interaction parameters obtained for three solvents with PIB at two different temperatures are shown in Table 5.1 and with SBR at four different temperatures are shown in Table 5.2.

The same parameters calculated for n-hexane at twelve different temperatures, for cyclohexane and benzene at five different temperatures with Antishock Polystyrene are shown in Tables 5.3 and 5.4.

The results of the diffusion coefficient experiments for three different solvents with SBR and Antishock Polystyrene at three different temperatures are given in Tables 5.5 and 5.6. The diffusion coefficients for three different solvents with PIB at 313.1 K are also given in Table 5.7.

Heat of solution obtained for Antishock Polystyrene in the temperature range of 382.3 K-394.1 K and for SBR in the temperature range of 343.3K-363.2 K are shown in Table 5.8.

The values of χ^* obtained for PIB by using hard core volumes for 10 % loading are given in Table 5.1. χ^* values of this study are compared with those given in literature (14, 27, 28). During the calculation of χ^* by Eq.(3.15), V_1^* and V_2^* volumes were obtained from Bonner and Prausnitz (29). χ^* values of this study agree quite well with those obtained by Newman and Prausnitz(27). As seen in Table 5.1, χ^* values are greater than χ values and cyclohexane has the lowest Flory Huggins parameter values among the solvents investigated. This implies that cyclohexane is the most suitable solvent for PIB.

If Flory Huggins parameters and infinite dilution activity coefficients for Antishock Polystyrene and SBR in Tables 5.2-5.4 are examined benzene appears to have the lowest value of χ and Ω_1^∞ , hence it is the most suitable solvent for both Antishock Polystyrene and SBR.

As it can be seen from Tables 5.1-5.4 χ and Ω_1^∞ are both functions of temperatures. As the temperature increase Flory Huggins parameter and infinite dilution activity coefficient both decrease.

Plots of χ against temperature for Antishock Polystyrene using n-hexane, benzene and cyclohexane are shown in Fig.5.1. It is evident that all systems exhibit similar type of behaviour. In particular, all plots show a positive minimum and curvature which remains positive throughout the range of temperatures investigated.

Over the years, a number of different expressions have been derived to predict the relationship between χ and temperature. A partial explanation of the exhibition of minima in χ vs T plots is given by Patterson and Kuwahara (30). χ is expressed as follows(30):

$$\chi = - (U/RT)v^2 + (C_p/2R)\tau^2 \quad (5.1)$$

where $-U$ is the energy of vaporization of the solvent, C_p is the configurational heat capacity, and R is the gas constant. The parameter v is related to the difference of cohesive energy and size between the solvent molecule and polymer segments. The τ parameter reflects the free volume change which occurs on mixing the dense polymer with solvent and is defined as:

TABLE 5.1

COMPARISON OF χ^* VALUES[§] OF PIB WITH THOSE IN LITERATURE (27)

Solvents	V_g^0 (ml g ⁻¹)	<u>T = 313.1 K</u>			
		Ω_1^∞	χ	χ^*	χ^* (lit)
Benzene	191.18	6.35	0.82	0.93	0.96
Cyclohexane	229.48	4.90	0.45	0.53	0.54
n-Pentane	39.04	7.46	0.68	0.77	0.80
<u>T = 323.1 K</u>					
Benzene	131.40	6.36	0.80	0.91	0.92
Cyclohexane	157.97	4.90	0.43	0.52	0.53
n-Pentane	29.19	7.42	0.65	0.76	0.79

§ Based on segment fraction

TABLE 5.2

 V_g^0 , Ω_1^∞ , χ VALUES OF SOLVENTS WITH SBR

AT VARIOUS TEMPERATURES

Solvents	Temp (K)	V_g^0 (ml g ⁻¹)	Ω_1^∞	χ
Benzene	343.3	95.94	4.23	0.33
	353.1	74.44	4.04	0.27
	358.3	63.92	4.03	0.26
	363.2	55.01	4.02	0.25
Cyclohexane	343.3	58.06	6.58	0.66
	353.1	43.60	6.48	0.63
	358.3	37.94	6.43	0.61
	363.2	32.57	6.43	0.60
n-Hexane	343.3	26.46	10.34	0.94
	353.1	19.98	10.00	0.90
	358.3	16.35	9.24	0.80
	363.2	14.41	9.03	0.77

TABLE 5.3

 V_g^0 , Ω_1^∞ , χ VALUES OF n-HEXANE WITH ANTISHOCK-POLYSTYRENE

AT VARIOUS TEMPERATURES

<u>Temp</u> (K)	<u>V_g^0</u> (ml g ⁻¹)	<u>Ω_1^∞</u>	<u>χ</u>
313.3	46.96	15.36	1.41
323.2	33.43	15.16	1.38
328.3	28.09	15.01	1.36
333.1	24.74	14.82	1.34
343.3	18.50	14.78	1.32
353.1	13.92	14.50	1.28
363.2	12.48	11.87	1.06
373.3	11.73	9.84	0.85
382.3	9.37	9.67	0.81
390.3	7.70	10.34	0.87
394.1	6.81	11.04	0.92
402.3	5.47	11.26	0.93

TABLE 5.4

 V_g^0 , Ω_1^∞ , χ VALUES OF SOLVENTS WITH ANTISHOCK POLYSTYRENE

AT VARIOUS TEMPERATURES

Solvents	Temp (K)	V_g^0 (mlg ⁻¹)	Ω_1^∞	χ
Benzene	363.3	48.24	4.58	0.40
	373.3	44.24	3.73	0.18
	385.2	34.77	3.72	0.16
	388.2	30.57	3.86	0.19
	396.6	24.98	4.19	0.26
Cyclohexane	363.3	25.46	8.24	0.87
	373.3	24.52	6.48	0.62
	385.2	19.32	6.30	0.57
	388.2	16.62	6.84	0.65
	396.6	14.10	7.18	0.69

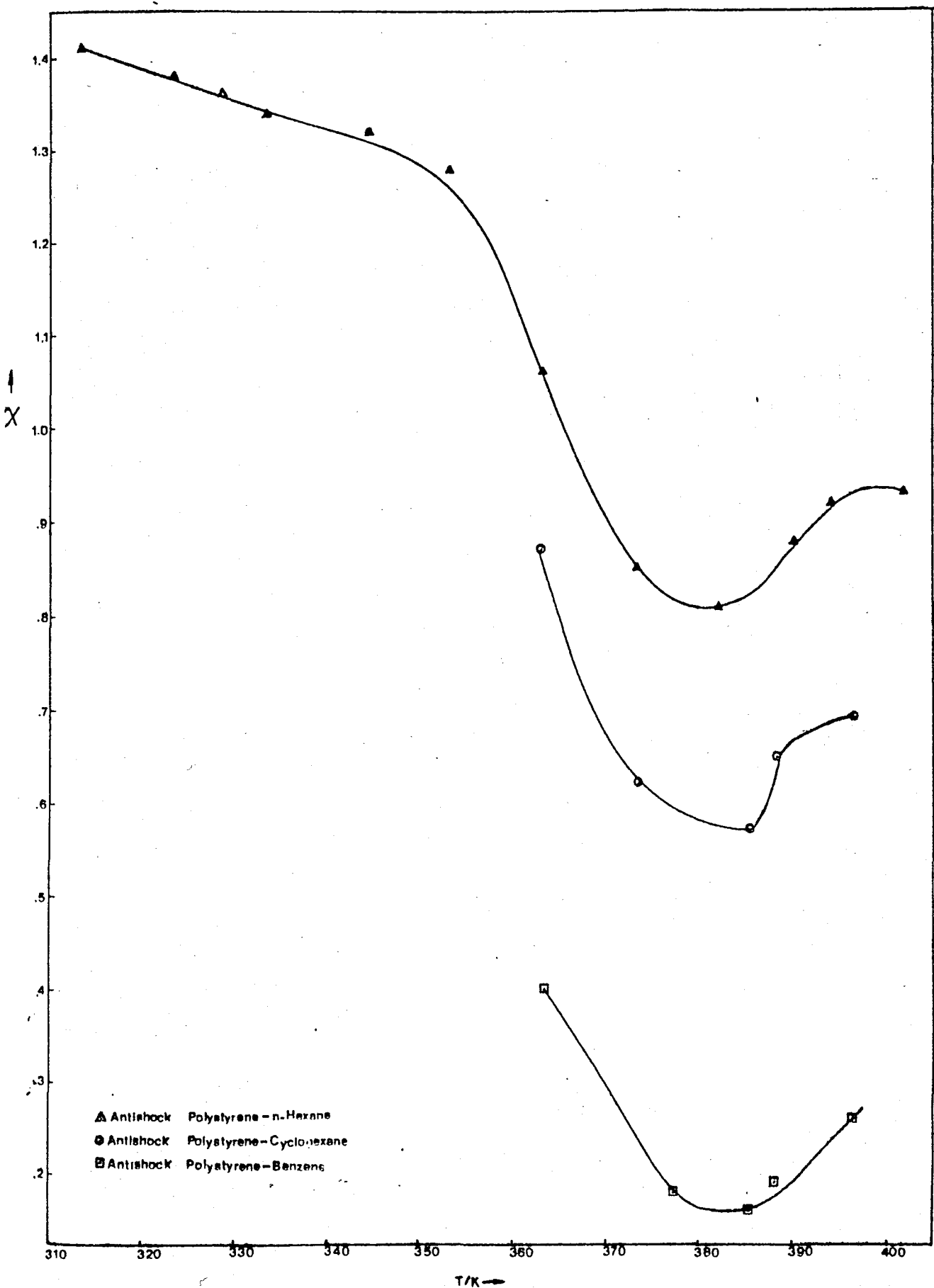


Fig. 5.1. Plots of χ against temperature for solvent-Antishock Polystyrene binary systems

$$\tau = 1 - (T_1^* / T_2^*) \quad (5.2)$$

where T_1^* and T_2^* are the characteristic temperature reduction parameters of the solvent and polymer, respectively.

The variation of the two terms on the right-hand side of Eq.(5.1) with temperature has been discussed by Patterson and Kuwaraha (30) who conclude that the first term, which represents the contact energy dissimilarity and is positive, should decrease with an increase in temperature, while the second term, reflecting the free volume dissimilarity should increase without limit. This situation would clearly allow a plots of λ vs T to show a minimum.

Glass transition curves for Antishock Polystyrene were determined by using GLC technique. n-Hexane was used injected to the column at twelve different temperatures selected in the temperature range of 313.3 K- 402.3K Benzene and cyclohexane were also injected in the temperature range 363.3 K- 396.6 K. It is reported that (32,33) heterogeneous polymer systems such as high impact polystyrene (antishock polystyrene) exhibit glass transitions for each of the individual polymers present although some shifting and broadening are almost observed as well. Therefore Antishock Polystyrene reveals its heterogeneous nature by showing the two distinct damping peaks i.e., the rubber peak -80°C to -95°C and the polystyrene peak at about 80°C to 90°C .As it seen from Fig.5.2 glass transition temperature was observed for n-hexane as solvent was based on the study of the Braun and Guillet(20). They have shown that both solvent and nonsolvent probes should be appropriate for such experiments.

Braun and Guillet (19) have also shown that the temperature of first deviation from the normal linear behaviour due to surface adsorption is essentially unaffected by coating thickness. The considerable changes in the shape of the retention diagrams are brought about by changing the surface to volume ratio of the stationary phase. If too low a coating thickness or an inert support of verry high surface area is used, this change of retention mechanism may no longer be detectable. In this study, 10 % loading was chosen so the deviation from linearity was quite detectable as shown Fig. 5.2.

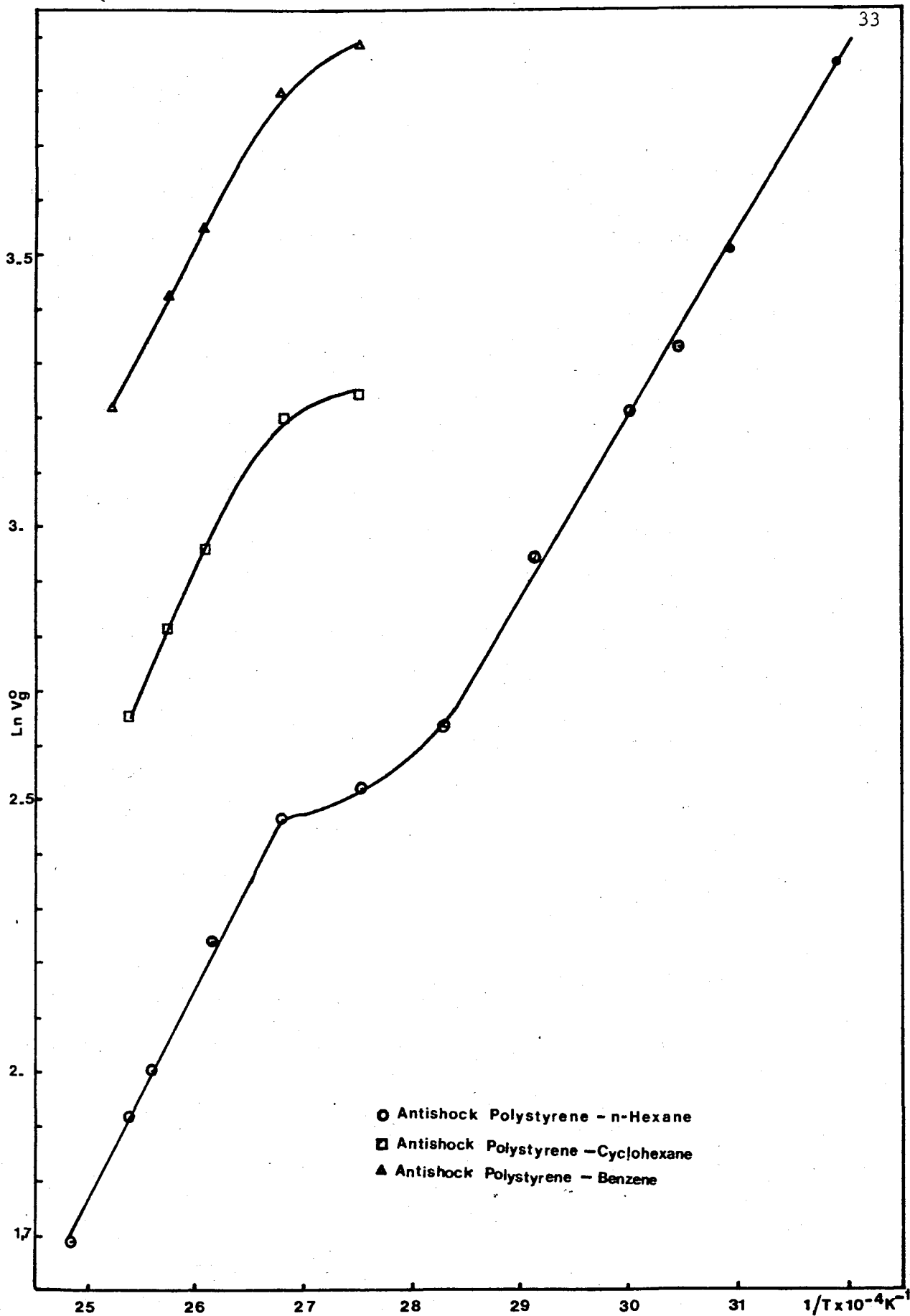


Fig.5.2. Glass transition curve of Antishock Polystyrene using n-Hexane

The results of the diffusion coefficients are given in Tables 5.5 to 5.7 and Fig.5.3-5.4. The numerical value of the partition ratio k and slope of curve (C) were also included in the tables at all temperatures. The results of a series of experiments to measure the amount of peak spreading as a function of flow rate are shown in Figs.5.3-5.4. When sufficiently slow flow rates are employed, the plate heights can be seen to pass through a minimum, as predicted by the Van Deemter Eq.(3.18). At higher flow rates, H increases linearly with u , with gradient C given by the simple Van Deemter expression.

Comparison of these values with those obtained using conventional techniques (e.g.sorption,permiation) are complicated by the different areas of applicability of the methods. At any given temperature, the gas chromatographic method gives results with small concentrations of diffusants of rather lower volatility than is usual in sorption and permeation experiments.The gas chromatographic method requires a uniform polymer layer of known thickness, for practical reasons this requires a relatively small loading of polymer in the column so that less volatile diffusants must be used to increase retention times. On the other hand sorption or permeation experiments are normally performed with relatively high vapor pressure of diffusant. Thus for comparison, data at zero diffusant concentration are required for systems where the polymer and diffusant type and temperature range are convenient for gas chromatography. Gray and Guillet (8) have reported data on the diffusion coefficients for benzene and n-decane in low density polyethylene by GLC.For polyethylene-benzene system at 25°C, the value of D_1 of $0.82 \times 10^{-8} \text{ cm}^2\text{sec}^{-1}$ and polyethylene-n-decane system at 80°C the resultant value of D_1 of $1.34 \times 10^{-8} \text{ cm}^2\text{sec}^{-1}$ were found. These values do not help us much to make any comparison but give an idea of the order of magnitude of diffusion coefficients.

The gas chromatographic measurement of diffusion rates appears to complement the usual sorption and permeation methods, as diffusion at low penetrant concentrations. However, use of the simple Van Deemter equation to interpret the gas chromatographic data may only be valid for relatively nonpolar penetrants and polymers at temperatures well above the glass transition temperature of the polymer. Otherwise, strong polymer-penetrant interactions may result in thermodynamic peak spreading and thus a diffusion

TABLE 5.5

DIFFUSION COEFFICIENTS OF SOLVENTS WITH SBR

AT VARIOUS TEMPERATURES

Solvents	Temp. (K)	Van Deemter [§] c term (sec x 10 ³)	k [§]	D ₁ [§] (cm ² sec ⁻¹ x10 ⁷)
Benzene	343.3	4.7 ± 0.1	7.0	4.2
	353.1	4.2 ± 0.9	4.9	6.1
	363.1	2.9 ± 0.1	4.0	9.8
Cyclohexane	343.3	9.8 ± 0.9	4.2	2.9
	353.1	10.5 ± 1.0	3.2	3.2
	363.1	14.5 ± 0.1	2.7	3.7
n-Hexane	343.3	18.9 ± 0.1	1.8	2.2
	353.1	18.3 ± 0.2	1.4	2.4
	363.1	16.0 ± 0.1	1.3	2.8

§ See Eqs. (3.20) and (3.21)

TABLE 5.6

DIFFUSION COEFFICIENTS OF SOLVENTS WITH ANTISHOCK POLYSTYRENE
AT VARIOUS TEMPERATURES

Solvents	Temp. (K)	Van Deemter c term (sec x 10 ³)	k	D ₁ (cm ² sec ⁻¹ x10 ⁸)
Benzene	382.3	59. ± 0.2	2.3	6.4
	394.1	53. ± 2.0	2.0	7.7
	402.3	49. ± 1.0	1.6	8.8
Cyclohexane	382.3	77. ± 1.0	1.3	5.7
	394.1	76. ± 3.0	1.2	6.0
	402.3	66. ± 1.0	1.0	6.9
n-Hexane	382.3	81. ± 0.6	0.6	5.3
	394.1	69. ± 0.5	0.5	5.9
	402.3	60. ± 2.0	0.4	6.2

TABLE 5.7

DIFFUSION COEFFICIENTS OF SOLVENTS WITH PIB AT 313.1 K

Solvents	Van Deemter c term (sec x 10 ³)	k	D ₁ (cm ² sec ⁻¹ x10 ⁸)
Benzene	49. ± 0.1	10.6	2.9
Cyclohexane [§]	45. ± 0.3	9.5	3.5
n-Pentane	157. ± 0.2	2.2	2.5

§ 316.3 K

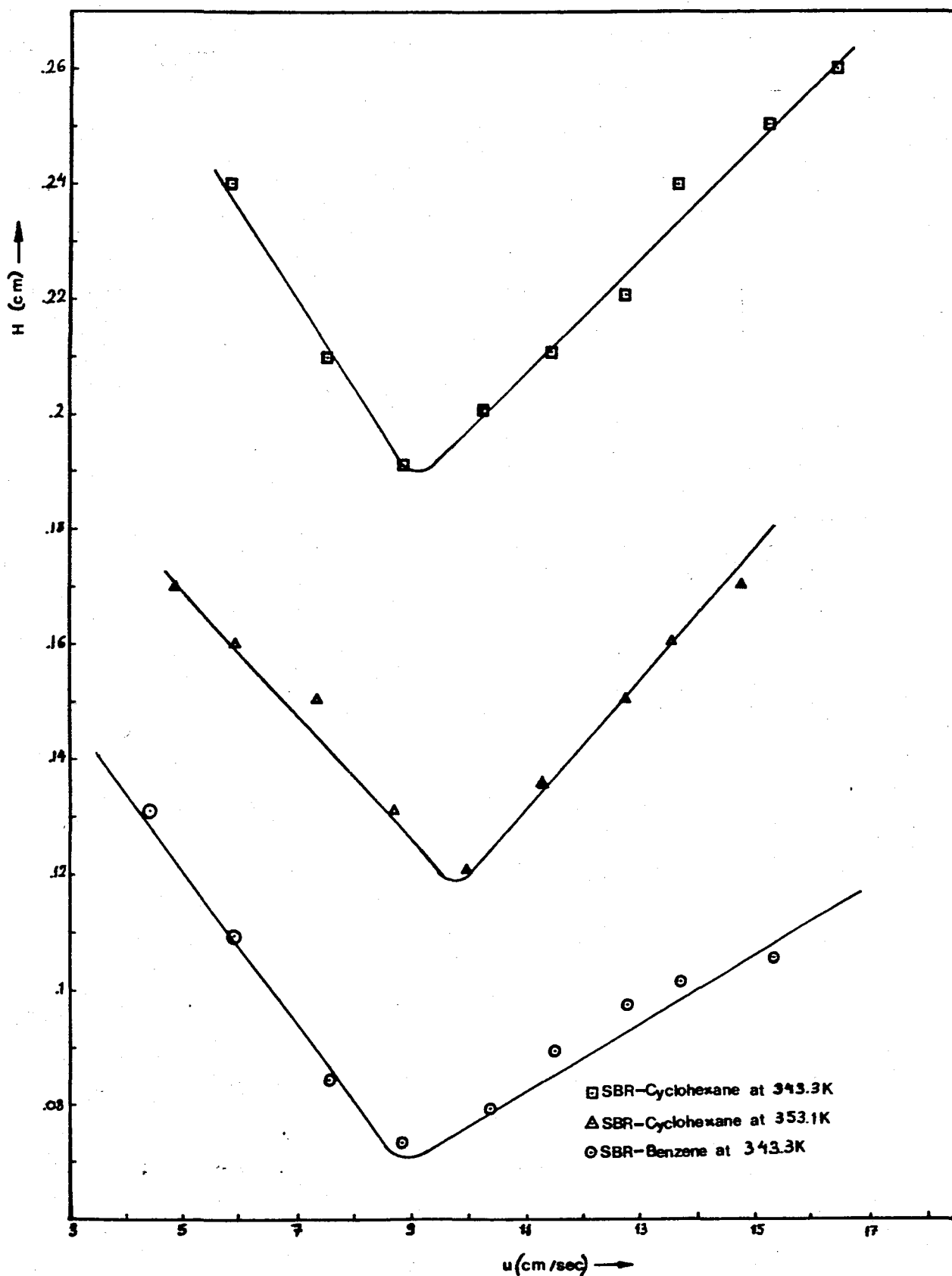


Fig. 5.3. Van Deemter curves for SBR-solvent systems

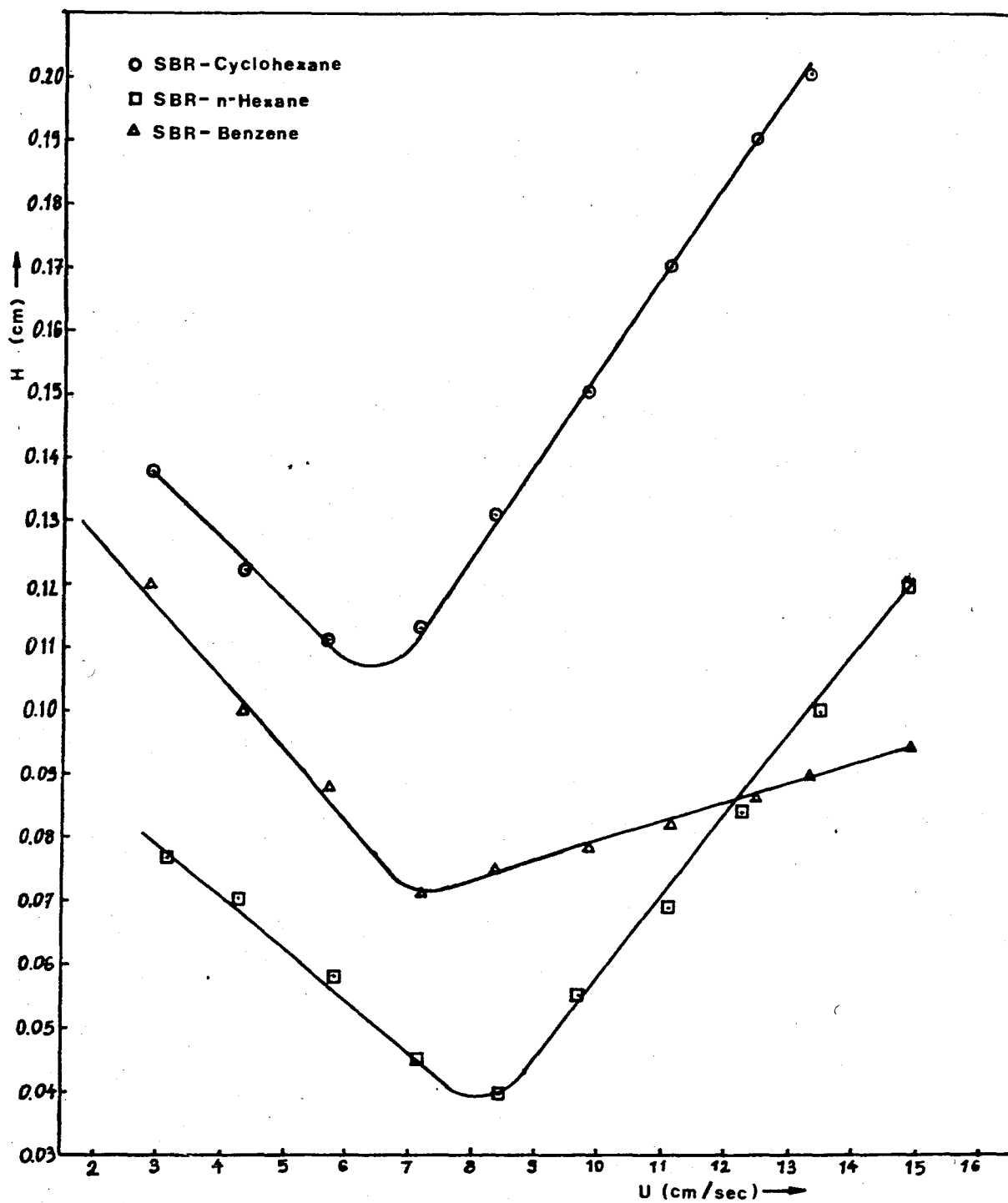


Fig. 5.4. Van Deemter curves for SBR-solvent systems at 363.1 K

TABLE 5.8

HEATS OF SOLUTION ($-\Delta H_s$ kcal/mole) OF VARIOUS
SOLVENTS WITH ANTISHOCK POLYSTYRENE AND SBR

<u>Solvents</u>	<u>polymers</u>	<u>Temp. Range (K)</u>	<u>$-\Delta H_s$ (kcal/mole)[§]</u>
Benzene	Antishock Polystyrene	382.3-390.4-394.1	8.4
Cyclohexane	"	"	11.4
n-Hexane	"	382.3-390.4-394.1-402.3	8.4
Benzene	SBR	343.3-353.1-358.3-363.2	6.9
Cyclohexane	"	"	7.1
n-Hexane	"	"	7.6

§ Correlation coefficients of all ΔH_s values given in this column are 0.99 .

coefficient which is dependent on both time and penetrant concentration. In this study the selected solvents and polymers are all nonpolar. Therefore the thermodynamic peak spreading can be discarded.

Effect of carrier gas flow rate on specific retention volume data was observed by taking retention data at various gas flow rates. The retention volumes measured in the nonequilibrium region (region II in Fig. 3.1) shows a drastic dependence on the flow rate of carrier gas. Fig. 5.5 shows the retention volumes measured for n-hexane-antishock polystyrene system at three or four different flow rates. Retention volumes become highly flow rate dependent in the nonequilibrium region, as seen by the curves marked as 3, 4 and 5 in Fig. 5.5. These data were extrapolated to zero flow rate. For equilibrium region (region III in Fig. 3.1) retention volumes slightly dependent on flow rates as shown in curves marked as 1 and 2 in Fig. 5.5. In this study for antishock polystyrene, data were taken both in equilibrium and nonequilibrium region, for SBR in equilibrium region and for PIB in nonequilibrium region. For more accurate results, the extrapolation of measured retention volumes to zero flow rate extends the linear region associated with equilibrium bulk sorption over a wider temperature range.

The origin of the flow rate dependence of retention volumes for bulk sorption was investigated by Braun and Guillet (31). Since nonequilibrium is attributed to the slow diffusion of solvent molecules in stationary phase, a change of carrier gas flow rate affects the rate of movement of a band of solvent through the column and the "residence time" over the stationary phase. As the flow rate is decreased, the polymer-solvent system is allowed to come closer to or even reach equilibrium, leading to larger specific retention volumes.

The heats of solution obtained for SBR and Antishock Polystyrene with various solvents are shown in Table 5.8. The linear regression technique was used to determine the heats of solution in the given temperature range for the linear portion of the curves obtained in the equilibrium region (region III in Fig. 3.1). Since heats of solution for antishock polystyrene and SBR could not be found in the literature, a detailed comparison of the values calculated in this work with those in references could not be made.

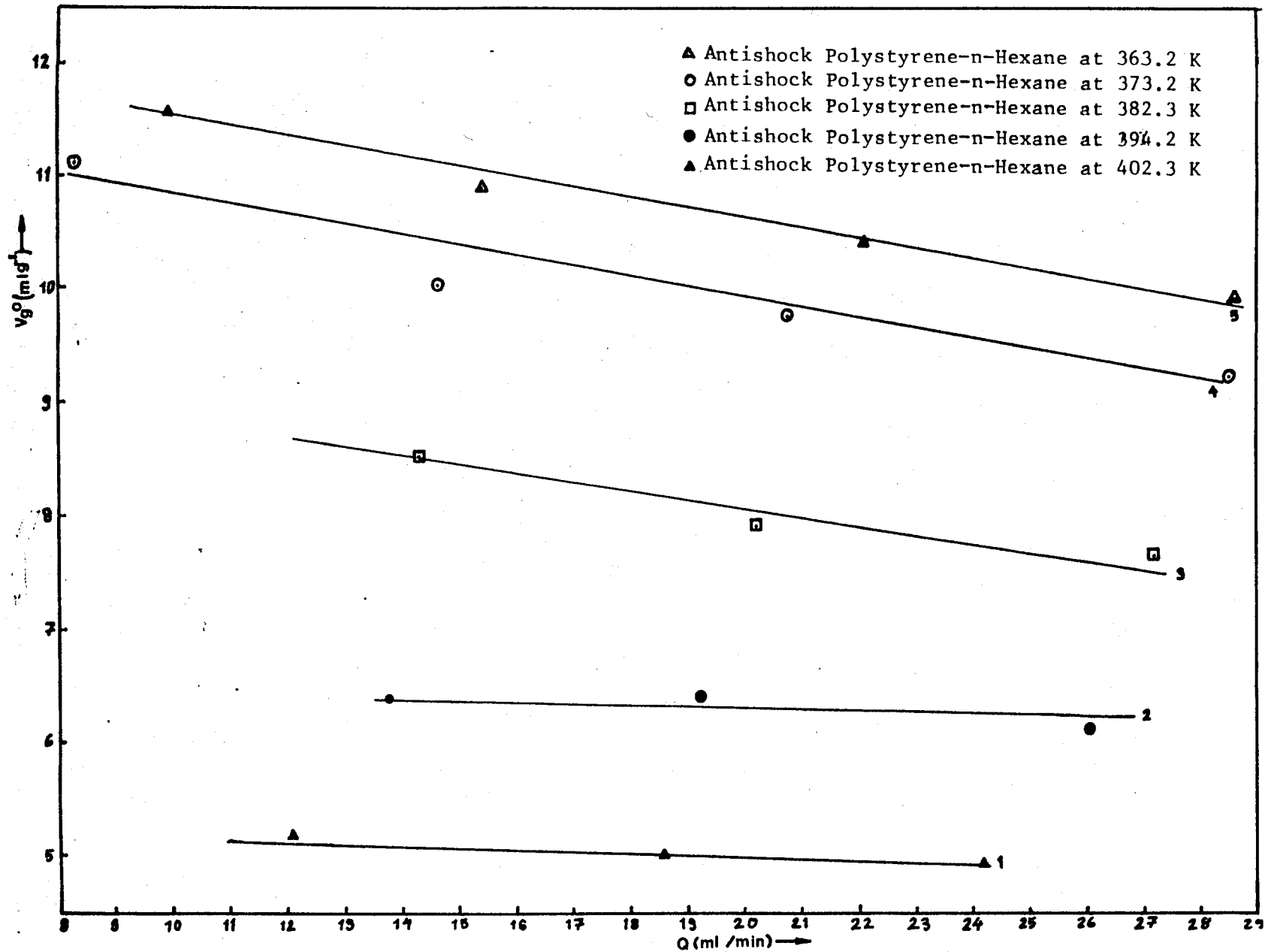


Fig. 5.5. Effect of gas flow rate on retention data for the column packed with Antishock Polystyrene

6. CONCLUSION AND RECOMMENDATIONS

6.1 Conclusions

In this study useful thermophysical properties such as Flory-Huggins interaction parameter, weight fraction infinite dilution activity coefficient and heat of solution were obtained for PIB, SBR and Antishock Polystyrene with four different nonpolar solvents namely benzene, cyclohexane, n-hexane and n-pentane at different temperatures. In addition, diffusion coefficients of these solvents with the same polymers were determined. Such parameters have uses in various industrial applications. For example, one of the crucial problems of the polymer industry is the removal of small amounts of volatile residuals to meet environmental, health and safety regulations. This concern with polymer purification has initiated a renewed interest in the area of molecular diffusion of solvent in molten polymers. Also in the drying of polymer film coatings, it is necessary to know the volatility (vapor pressure) of the solvent over the coating film at small solvent concentrations. This volatility can be used to calculate the equilibrium solvent content of a polymer film during the drying process.

The results of the diffusion coefficient experiments reveal that when polymers are coated evenly on spherical beads, reasonable values for penetrant diffusion coefficients can be calculated, using the simple Van Deemter equation from measurements of gas chromatographic peak width as a function of carrier gas flow rate.

In conclusion, such parameters obtained by GLC, apart from their use in theoretical studies, have been used in various industrial applications. It is possible to predict volatilities, solubilities and diffusion of penetrants by using only small amounts of polymer and solvents.

6.2 Recommendations

For further work the following are recommended:

1. Coating of beads with rubbers (especially SBR) proved quite difficult when the beads were placed in a benzene solution of rubber, and the solvent evaporated by gently heating and stirring, the rubber didnot adhere uniformly to the bead surfaces. A better method or other materials should be used to coat the beads with rubbers.
2. Injection of the diffusant "probes" onto the columns must be performed (if it is possible) using on automatic vapor injection system. Then this system will avoid variations in the output peak shapes due to nonuniform liquid injection sizes and evaporation rates.

LITERATURE CITED

1. Dinçer, S., Boğaziçi Üniversitesi Dergisi, 4-5, 1 (1977).
2. Dwyer, J., Karim, A.K., Ind.Eng.Chem.Fundam., 14, 196 (1975).
3. Guillet, J.E., J.Macromol.Sci., Macromol. Chem., 4, 1669 (1970).
4. Newman, R.D., Prausnitz, J.M., J.Paint Technol., 45, 34 (1973).
5. Purnell, H., "Gas Chromatography", Wiley, Newyork, 1962.
6. Flory, P.J., "Principles of Polymer Chemistry", Cornell Univ.Press, Ithaca, N.Y. 1953.
7. Guillet, J.E., "Progress on Gas Chromatography", Wiley, Newyork, 1973.
8. Braun, J.M., Poos, S., and Guillet, J.E., J.Polym. Sci., Polym. Lett. Ed., 14, 257 (1976).
9. Guillet, J.E., J.Macromol.Sci., Macromol.Chem., A4, 1669 (1970).
10. Leslie, S., Zlatkis, A., "The Practice of Gas Chromatography", Wiley, Newyork, 1967.
11. Littlewood, A.B., "Gas Chromatography", Academic Press, Newyork, 1972.
12. Patterson, D., Tewari, Y.B., Schreiber, H.B., Guillet, J.E., Macromol., 4, 356 (1971).
13. Orwoll, R.A., Rubber Chem. Technol., 50, 451 (1977).
14. Patterson, D., Tewari, Y.B., Schreiber, H.P., Guillet, J.E., Macromol., 4, 356 (1971).
15. Blanks, R.F., Prausnitz, J.M., Ind.Eng.Chem., 3, 1 (1973).
16. Dinçer, S., Doçentlik Tezi, Boğaziçi University, Turkey, 1977 Eylül.
17. Braun, J.M., Guillet, J.E., Adv.Poly.sci., 21, 107 (1976).
18. Braun, J.M., Guillet, J.E., Macromolecules, 9, 617 (1976).
19. Braun, J.M., Lavoie, A., Guillet, J.E., Macromolecules, 6, 382 (1975).
20. Braun, J.M., Guillet, J.E., Macromolecules, 9, 340 (1976).
21. Harris, F.W., Seymour, R.B., "Structure-Solubility Relationships in Polymers", Academic Press, Newyork, 1977.
22. Meyer, E.F., J.Chem.Edu., 50, 191 (1973).
23. Gray, D.G., Guillet, J.E., Macromolecules, 6, 223 (1973).
24. Van Deemter, J.J., Zuiderweg, F.J., Klinkenberg, A., Chem.Eng.Sci., 5, 271 (1956).
25. Savaşçı, T., Personal Communication, PETKİM Petrokimya A.Ş., 1985.
26. "A User's Guide to Chromatography", Regis Chemiscal Company Press., Illinois, 1976.

27. Newman, R.D., Prausnitz, J.M., J.Physical Chemistry, 76, 10 (1972).
28. Leung, Y.K., Eichinger, B.E., J.Phy.Chemistry, 78, 1, (1974).
29. Bonner, D.C., Prausnitz, J.M., J.AIChE, 19, 5 (1973).
30. Patterson, D., J.Poly.Sci., Part C, 16, 3379 (1968).
31. Braun, J.M., Guillet, J.E., Macromolecules, 6, 882 (1975).
32. "Encyclopedia of Polymer Science and Technology", Vol.2,5,10, Interscience Div., N.Y., 1970.
33. Orhmer, K., "Encyclopedia of Chemical Technology", Vol.21, Interscience Div., N.Y., 1976.
34. Billmeyer, F.W., "Textbook of Polymer science", Wiley, New York, 1962.
35. Brydson, J.A., "Plastic Materials", Newnes-Butterworths, London, 1975.
36. Shirley, H.R., J.App.Polym.Sci., 18, 3305, (1974).
37. Shirley, H.R., J.App.Polym.Sci., 18, 3311, (1974).
38. Moore, J.W., "Physical Chemistry" Longman, London, 1972.
39. Reid, R.C., Sherwood, T.K., "The properties of Gases and Liquids", KcGrawHill, New York, 1966.
40. Dinger, S., Personal Communication, 1985.
41. Silverstein and Bassler, "Spectrometric Identification of Organic Compounds", Wiley, N.Y., 1963.
42. Rodriguez, "Principles of Polymer Systems", McGraHill, N.Y., 1970.

APPENDICES

APPENDIX 1- PRODUCTION AND USES OF POLYMERS USED IN THIS STUDY

APPENDIX 2- NUMBER AVERAGE MOLECULAR WEIGHT DETERMINATION BY MEMBRANE
OSMOMETER

APPENDIX 3- RAW EXPERIMENTAL DATA

APPENDIX 4- REQUIRED PHYSICAL PROPERTIES OF SOLVENTS

APPENDIX 5- SAMPLE CALCULATIONS

APPENDIX I

PRODUCTION AND USES OF POLYMERS USED IN THIS STUDY

SBR and antishock polystyrene are commercially available materials from PETKİM A.Ş. Turkey. However, antishock polystyrene used in this study is imported from Spain by Çavuşoğlu Plastik Sanayi.

A.1.1. Styrene-Butadiene Rubbers

Styrene-Butadiene rubbers contain 25 % styrene and 75 % butadiene. Production of SBR was begun in the United States during World War II. The rubber was made by emulsion polymerization. After the war, product quality was improved by carrying out the polymerization at 5°C or even at temperatures as low as -10°C or -18°C. These changes were brought about by the use of more active initiators such as cumene hydroperoxide and the addition of antifreeze components to the mixture. The product is known as "Cold Rubber". The cold SBR polymers produced at the lower temperature but stopped at 60 % conversion, at 5°C ; 60 % conversion to polymer occurs in about 12-15 hr. Cold SBR is superior to the standard product because it contains less low molecular-weight rubber, and a higher proportion (70-75 %) of the trans-1-4-configuration of polybutadiene.

The major use for SBR is for tires and tire products but cold SBR appears equal in most respects to natural rubber, especially for lighter-duty tire use. For many mechanical goods SBR is superior to natural rubber because of its easier processing and good quality end product. For example, it is used as belting hase, molded goods, unvulcanized sheet, flooring, wire and cable coatings (32,33).

A.1.2. Polyisobutylene

Polyisobutylene is derived from the monomer isobutylene. The polymerization of isobutylene is accomplished industrially by the application of low temperature cationic polymerization. Isobutylene polymerizes rapidly at -80°C with Friedel-Crafts catalysts. In a bulk system at -80°C , rapid polymerization is induced by bubbling BF_3 gas through isobutylene. Catalyst solution made by dissolving anhydrous aluminum chloride in methyl chloride is added. Polymer forms at once as a finely divided product suspended in the reaction mixture (32,34,35). About 75 % of the polyisobutylene rubber produced is used to produce inner tubes of tires.

A.1.3. Antishock Polystyrene

Antishock Polystyrene represents the class of rubber-modified styrene polymers. Rubber is incorporated into polystyrene primarily to impart toughness. These materials are commonly called impact polystyrenes and are available in many different varieties. Impact-resistant polystyrene has most of the advantages of polystyrene, such as rigidity, ease of fabrication, and variety of colors and granule sizes. Being two phase systems, they are not available in transparent forms (32). The supplied polymer is high impact polystyrene, opaque, in the form of white granules and contains about 5-10 % polybutadiene. High-impact polystyrene (HIPS) is conventionally prepared by bulk suspension or emulsion techniques (36,37). Bulk-suspension polymerization is a two-stage process in which polybutadiene is dissolved in styrene monomer and partially polymerized with the aid of catalysts. This pre-polymer (~ 15 % to 30 % conversion) is then added to water containing a suspending agent and the polymerization is completed.

The high impact polystyrene is available in high heat, easy flow and other formulations and are used for injection molding, extrusion and blow molding.

APPENDIX 2

NUMBER AVERAGE MOLECULAR WEIGHT DETERMINATION

BY MEMBRANE OSMOMETER

A.2.1. Membrane Osmometer

In this study the number average molecular weights of the polymers were determined by Herbert-Knauer electronic membrane osmometer, present at I.T.U. laboratories. The specifications of osmometer is given as :

Measuring range : 2.5/5/10/20/40 cm solvent column. Accuracy of Pressure Measurement : 0.5 % of the measuring range.

Operating Temperatures : Continuously adjustable between 20°C and 130°C on a ten turn helical potentiometer with 1000 scale graduation.

A.2.2. Operation of the Osmometer

The electronic membrane osmometer consists of a stainless steel measuring cell. This measuring cell is divided by a semi-permeable membrane. The pure solvent, which is connected by a capillary to an electronic pressure measuring system, is situated beneath the semi-permeable membrane. The upper side of the semi-permeable membrane can be rinsed with pure solvent or a solution. The pure solvent gives an osmotic pressure of 0. The indicator of the pressure measurement system is adjusted to 0 by means of the zero adjuster. Measurement is achieved by replacing the solvent on the upper side of the membrane with a solution. The solvent on the lower side of the membrane can diffuse through the membrane into solution while the solute molecules in the solution are retained by the membrane. A negative pressure in the lower cell is thereby produced, which corresponds to the osmotic pressure in the upper cell. This negative pressure is then measured by the electronic pressure measurement system.

In this study, the semipermeable membrane is regenerated cellulose and the solvent is toluene. This membrane is permeable to toluene but impermeable to polymer. If pure toluene is put on one side of a membrane and a solution of polymer-toluene on the other side, the requirements for osmosis are satisfied. Toluene flows through the membrane from the toluene rich to toluene poor side of the membrane. This flow continues until the chemical potential of the toluene is the same on both sides.

In dilute solutions the osmotic pressure Π obeys the relationship (38) :

$$\Pi = CRT \quad (A.2.1)$$

where $C = \frac{n}{V}$ is the molar concentration of solute. Here n is defined as :

$$n = \frac{m}{M_n} \quad (A.2.2)$$

If C is taken as the weight concentration of solute then the number average molecular weight (M_n) is given by :

$$M_n = \frac{RT}{\frac{\Pi}{C} \rho_{(C \rightarrow 0)}} \quad (A.2.3)$$

where ρ is the density of solute. The values for Π are divided by the corresponding solution concentration C and then plotted as a function of Π/C against solution concentration. The resulting curve is extrapolated to obtain Π/C value at zero concentration.

APPENDIX 3

RAW EXPERIMENTAL DATA

1. Data given in Tables A.3.1 - A.3.21 are for diffusion coefficient.
2. Data given in Tables A.3.22 - A.3.28 are for the calculation of retention volumes used to obtain χ, Ω^{∞} and ΔH_s .
3. Pressure given in Tables A.3.1 - A.3.21 presents gauge pressure.
4. Pressure given in Tables A.3.22 - A.3.28 represents absolute pressure.

TABLE A.3.1

DATA FOR PIB-n-PENTANE SYSTEM AT 313.1 K

<u>P</u> (kg/cm ²)	<u>Q</u> (ml/min)	<u>u</u> (cm/sec)	<u>t_R</u> (min)	<u>t_A</u> (min)	<u>w_{1/2}</u> (cm)	<u>H</u> (cm)
0.50	16.40	3.55	1.500	0.470	0.415	1.38
0.75	27.27	5.21	1.010	0.320	0.350	2.17
1.00	38.46	6.94	0.770	0.240	0.310	2.93
1.25	52.63	8.27	0.600	0.190	0.250	3.13
1.50	69.76	9.80	0.510	0.170	0.220	3.36
1.75	85.71	11.82	0.450	0.141	0.200	3.56
2.00	107.41	13.89	0.386	0.120	0.180	3.92
2.25	130.43	15.15	0.350	0.110	0.170	4.26
2.50	150.00	16.67	0.310	0.096	0.155	4.51

TABLE A.3.2

DATA FOR PIB-BENZENE SYSTEM AT 313.1 K

<u>P</u> (kg/cm ²)	<u>Q</u> (ml/min)	<u>u</u> (cm/sec)	<u>t_R</u> (min)	<u>t_A</u> (min)	<u>w_{1/2}</u> (cm)	<u>H</u> (cm)
0.50	16.22	3.62	5.77	0.460	1.190	0.77
0.75	26.54	5.38	3.89	0.310	0.895	0.97
1.00	40.00	6.67	2.89	0.250	0.720	1.12
1.25	52.63	8.33	2.42	0.200	0.635	1.24
1.50	69.76	9.80	1.97	0.170	0.550	1.32
1.75	85.71	11.90	1.57	0.140	0.440	1.42
2.00	107.41	13.89	1.48	0.120	0.430	1.52
2.25	130.43	15.15	1.36	0.110	0.400	1.56
2.50	150.00	16.67	1.23	0.100	0.370	1.62

TABLE A.3.3

DATA FOR PIB-CYCLOHEXANE SYSTEM AT 316.3 K

<u>P</u> (kg/cm ²)	<u>Q</u> (ml/min)	<u>u</u> (cm/sec)	<u>t_R</u> (min)	<u>t_A</u> (min)	<u>w_{1/2}</u> (cm)	<u>H</u> (cm)
2.50	136.36	15.38	1.16	0.108	0.450	2.72
2.25	115.38	13.89	1.23	0.120	0.470	2.63
2.00	100.00	12.90	1.41	0.129	0.535	2.60
1.75	78.94	10.75	1.61	0.155	0.600	2.51
1.50	69.76	9.80	2.03	0.170	0.750	2.46

TABLE A.3.4

DATA FOR SBR-n-HEXANE SYSTEM AT 343.3 K

<u>P</u> (kg/cm ²)	<u>Q</u> (ml/min)	<u>u</u> (cm/sec)	<u>t_R</u> (min)	<u>t_A</u> (min)	<u>w^{1/2}</u> (cm)	<u>H</u> (cm)
3.00	150.00	16.53	0.281	0.101	0.030	0.200
2.75	136.36	15.38	0.302	0.108	0.030	0.180
2.5	120.00	13.70	0.334	0.122	0.030	0.140
2.25	100.00	12.74	0.359	0.131	0.030	0.130
2.00	83.33	11.49	0.406	0.145	0.030	0.098
1.75	69.77	10.36	0.455	0.161	0.030	0.078
1.50	55.55	8.85	0.526	0.189	0.030	0.059
1.25	42.86	7.57	0.623	0.220	0.040	0.074
1.00	31.25	5.97	0.779	0.279	0.055	0.090
0.75	21.20	4.48	1.060	0.372	0.075	0.091

TABLE A.3.5

DATA FOR SBR-n-HEXANE SYSTEM AT 353.1 K

<u>P</u> (kg/cm ²)	<u>Q</u> (ml/min)	<u>u</u> (cm/sec)	<u>t_R</u> (min)	<u>t_A</u> (min)	<u>w_{1/2}</u> (cm)	<u>H</u> (cm)
2.75	130.43	14.81	0.259	0.112	0.025	0.170
2.50	111.11	13.60	0.284	0.122	0.025	0.140
2.25	96.77	12.74	0.311	0.131	0.025	0.120
2.00	78.95	11.30	0.347	0.147	0.025	0.094
1.75	65.22	10.05	0.387	0.166	0.025	0.075
1.50	50.85	8.66	0.456	0.192	0.025	0.054
1.25	40.00	7.33	0.542	0.227	0.030	0.055
1.00	29.41	5.88	0.675	0.283	0.040	0.063
0.75	20.72	4.88	0.865	0.342	0.055	0.072

TABLE A.3.6

DATA FOR SBR-n-HEXANE SYSTEM AT 363.1 K

<u>P</u> (kg/cm ²)	<u>Q</u> (ml/min)	<u>u</u> (cm/sec)	<u>t_R</u> (min)	<u>t_A</u> (min)	<u>w_{1/2}</u> (cm)	<u>H</u> (cm)
2.75	120.00	14.92	0.244	0.112	0.020	0.120
2.50	103.45	13.55	0.264	0.123	0.020	0.100
2.25	88.23	12.27	0.293	0.136	0.020	0.084
2.00	75.00	11.11	0.322	0.150	0.020	0.069
1.75	61.22	9.71	0.366	0.172	0.020	0.055
1.50	49.18	8.47	0.417	0.197	0.020	0.040
1.25	33.22	7.14	0.503	0.233	0.025	0.045
1.00	27.91	5.79	0.616	0.287	0.035	0.058
0.75	19.05	4.36	0.804	0.382	0.055	0.070
0.50	12.00	3.06	1.150	0.545	0.075	0.077

TABLE A.3.7

DATA FOR SBR-CYCLOHEXANE SYSTEM AT 343.3 K

<u>P</u> (kg/cm ²)	<u>Q</u> (ml/min)	<u>u</u> (cm/sec)	<u>t_R</u> (min)	<u>t_A</u> (min)	<u>w_{1/2}</u> (cm)	<u>H</u> (cm)
3.00	150.00	16.53	0.513	0.101	0.062	0.260
2.75	136.36	15.38	0.557	0.108	0.065	0.250
2.50	120.00	13.70	0.610	0.122	0.070	0.240
2.25	100.00	12.74	0.676	0.131	0.075	0.220
2.00	83.33	11.49	0.743	0.145	0.081	0.210
1.75	69.77	10.36	0.840	0.161	0.090	0.200
1.50	55.55	8.85	0.972	0.189	0.100	0.190
1.25	42.86	7.57	1.150	0.220	0.125	0.210
1.00	31.30	5.97	1.440	0.279	0.165	0.240

TABLE A.3.8

DATA FOR SBR-CYCLOHEXANE SYSTEM AT 353.1 K

<u>P</u> (kg/cm ²)	<u>Q</u> (ml/min)	<u>u</u> (cm/sec)	<u>t_R</u> (min)	<u>t_A</u> (min)	<u>w_{1/2}</u> (cm)	<u>H</u> (cm)
2.75	130.43	14.81	0.458	0.112	0.045	0.170
2.50	111.11	13.60	0.499	0.122	0.047	0.160
2.25	96.77	12.74	0.547	0.131	0.050	0.150
2.00	78.95	11.30	0.604	0.147	0.052	0.135
1.75	65.22	10.05	0.680	0.166	0.055	0.120
1.50	50.85	8.66	0.797	0.192	0.068	0.131
1.25	40.00	7.33	0.945	0.227	0.087	0.150
1.00	29.41	5.88	1.170	0.283	0.110	0.160
0.75	20.72	4.88	1.500	0.342	0.145	0.170

TABLE A.3.9

DATA FOR SBR-CYCLOHEXANE SYSTEM AT 363.1 K

<u>P</u> (kg/cm ²)	<u>Q</u> (ml/min)	<u>u</u> (cm/sec)	<u>t_R</u> (min)	<u>t_A</u> (min)	<u>w_{1/2}</u> (cm)	<u>H</u> (cm)
2.50	103.45	13.33	0.397	0.124	0.042	0.200
2.25	88.23	12.50	0.474	0.133	0.048	0.190
2.00	75.00	11.17	0.535	0.149	0.052	0.170
1.75	61.22	9.90	0.603	0.168	0.055	0.150
1.50	49.59	8.40	0.691	0.193	0.059	0.130
1.25	38.22	7.19	0.820	0.230	0.065	0.113
1.00	27.39	5.74	1.020	0.290	0.075	0.111
0.75	19.04	4.36	1.340	0.382	0.090	0.122
0.50	11.41	2.98	2.000	0.560	0.200	0.138

TABLE A.3.10

DATA FOR SBR-BENZENE SYSTEM AT 343.3 K

<u>P</u> (kg/cm ²)	<u>Q</u> (ml/min)	<u>u</u> (cm/sec)	<u>t_R</u> (min)	<u>t_A</u> (min)	<u>w_{1/2}</u> (cm)	<u>H</u> (cm)
3.00	150.00	16.53	0.780	0.101	0.060	0.107
2.75	136.36	15.38	0.851	0.108	0.065	0.105
2.50	120.00	13.69	0.933	0.122	0.075	0.101
2.25	100.00	12.74	1.020	0.131	0.075	0.097
2.00	83.33	11.49	1.140	0.145	0.080	0.089
1.75	69.77	10.36	1.280	0.161	0.085	0.079
1.50	55.55	8.85	1.490	0.189	0.095	0.073
1.25	42.86	7.57	1.750	0.220	0.120	0.084
1.00	31.25	5.97	2.190	0.279	0.170	0.109
0.75	21.20	4.48	2.930	0.372	0.250	0.131

TABLE A.3.11

DATA FOR SBR-BENZENE SYSTEM AT 353.1 K

<u>P</u> (kg/cm ²)	<u>Q</u> (ml/min)	<u>u</u> (cm/sec)	<u>t_R</u> (min)	<u>t_A</u> (min)	<u>w_{1/2}</u> (cm)	<u>H</u> (cm)
3.00	150.00	17.36	0.623	0.096	0.050	0.120
2.75	130.43	14.81	0.674	0.112	0.053	0.110
2.50	111.11	13.60	0.740	0.122	0.056	0.103
2.25	96.77	12.74	0.805	0.131	0.060	0.100
2.00	78.95	11.30	0.896	0.147	0.065	0.094
1.75	65.22	10.05	1.000	0.166	0.070	0.088
1.50	50.85	8.66	1.170	0.192	0.080	0.084
1.25	40.00	7.33	1.360	0.277	0.100	0.098
1.00	29.41	5.88	1.730	0.283	0.140	0.118
0.75	20.72	4.88	2.250	0.342	0.195	0.136

TABLE A.3.12

DATA FOR SBR-BENZENE SYSTEM AT 363.1 K

<u>P</u> (kg/cm ²)	<u>Q</u> (ml/min)	<u>u</u> (cm/sec)	<u>t_R</u> (min)	<u>t_A</u> (min)	<u>w_{1/2}</u> (cm)	<u>H</u> (cm)
2.75	120.00	14.92	0.553	0.112	0.040	0.094
2.50	103.45	13.33	0.607	0.124	0.043	0.090
2.25	88.23	12.50	0.666	0.133	0.046	0.086
2.00	75.00	11.17	0.744	0.149	0.050	0.082
1.75	61.22	9.90	0.837	0.168	0.055	0.078
1.50	49.59	8.40	0.963	0.193	0.062	0.075
1.25	38.22	7.19	1.150	0.232	0.072	0.071
1.00	27.39	5.75	1.420	0.290	0.100	0.088
0.75	19.04	4.37	1.870	0.382	0.140	0.100
0.50	11.41	2.98	2.900	0.560	0.235	0.120

TABLE A.3.13

DATA FOR ANTISHOCK POLYSTYRENE-BENZENE SYSTEM AT 382.3 K

<u>P</u> (kg/cm ²)	<u>Q</u> (ml/min)	<u>u</u> (cm/sec)	<u>t_R</u> (min)	<u>t_A</u> (min)	<u>w_{1/2}</u> (cm)	<u>H</u> (cm)
3.00	90.91	11.17	0.499	0.149	0.110	0.880
2.50	67.41	9.26	0.602	0.180	0.125	0.780
2.25	57.09	8.44	0.652	0.197	0.130	0.720
2.00	48.39	7.55	0.725	0.221	0.140	0.670
1.75	39.47	6.78	0.830	0.246	0.150	0.630
1.50	32.26	5.88	0.952	0.283	0.170	0.580
1.25	24.69	4.91	1.130	0.339	0.190	0.510

TABLE A.3.14

DATA FOR ANTISHOCK POLYSTYRENE-BENZENE SYSTEM AT 394.1 K

<u>P</u> (kg/cm ²)	<u>Q</u> (ml/min)	<u>u</u> (cm/sec)	<u>t_R</u> (min)	<u>t_A</u> (min)	<u>w_{1/2}</u> (cm)	<u>H</u> (cm)
3.25	100.33	11.98	0.421	0.139	0.085	0.740
2.75	77.92	10.10	0.500	0.165	0.095	0.650
2.50	65.93	9.13	0.552	0.182	0.100	0.590
2.25	55.55	8.33	0.604	0.200	0.105	0.540
2.00	47.62	7.66	0.664	0.217	0.110	0.490
1.75	38.46	6.60	0.695	0.252	0.110	0.450
1.50	31.58	5.71	0.754	0.293	0.115	0.420

TABLE A.3.15

DATA FOR ANTISHOCK POLYSTYRENE-BENZENE SYSTEM AT 402.3 K

<u>P</u> (kg/cm ²)	<u>Q</u> (ml/min)	<u>u</u> (cm/sec)	<u>t_R</u> (min)	<u>t_A</u> (min)	<u>w₂</u> (cm)	<u>H</u> (cm)
3.50	29.7	12.34	0.362	0.135	0.057	0.450
3.25	36.58	11.56	0.371	0.144	0.057	0.420
3.00	45.45	10.75	0.440	0.155	0.057	0.350
2.75	54.05	10.15	0.423	0.164	0.057	0.320
2.50	63.42	9.05	0.490	0.184	0.058	0.250
2.25	75.00	8.29	0.542	0.200	0.060	0.220
2.00	83.80	7.41	0.593	0.225	0.062	0.190
1.75	96.77	6.51	0.677	0.256	0.065	0.160
1.50	109.09	5.63	0.774	0.296	0.067	0.130

TABLE A.3.16

DATA FOR ANTISHOCK POLYSTYRENE-CYCLOHEXANE SYSTEM AT 382,3 K

<u>P</u> (kg/cm ²)	<u>Q</u> (ml/min)	<u>u</u> (cm/sec)	<u>t_R</u> (min)	<u>t_A</u> (min)	<u>w_{1/2}</u> (cm)	<u>H</u> (cm)
3,00	90,91	11,17	0,338	0,149	0,110	1,91
2,50	67,41	9,26	0,403	0,180	0,120	1,74
2,25	57,69	8,44	0,441	0,197	0,135	1,69
2,00	48,39	7,55	0,490	0,221	0,145	1,62
1,75	39,47	6,78	0,555	0,246	0,170	1,59
1,25	24,69	4,91	0,786	0,339	0,210	1,41

TABLE A.3.17

DATA FOR ANTISHOCK POLYSTYRENE-CYCLOHEXANE SYSTEM AT 394.1 K

<u>P</u> (kg/cm ²)	<u>Q</u> (ml/min)	<u>u</u> (cm/sec)	<u>t_R</u> (min)	<u>t_A</u> (min)	<u>w₂</u> (cm)	<u>H</u> (cm)
3.00	90.91	10.81	0.328	0.154	0.085	1.21
2.75	77.92	10.10	0.357	0.165	0.090	1.15
2.50	65.93	9.13	0.397	0.182	0.097	1.07
2.25	55.55	8.33	0.442	0.200	0.107	1.05
2.00	47.62	7.66	0.492	0.217	0.120	1.01
1.75	38.46	6.60	0.547	0.252	0.125	0.94
1.50	31.58	5.71	0.624	0.293	0.130	0.78

TABLE A.3.18

DATA FOR ANTISHOCK POLYSTYRENE-CYCLOHEXANE SYSTEM AT 402.3 K

<u>P</u> (kg/cm ²)	<u>Q</u> (ml/min)	<u>u</u> (cm/sec)	<u>t_R</u> (min)	<u>t_A</u> (min)	<u>w_{1/2}</u> (cm)	<u>H</u> (cm)
3.50	109.09	12.34	0.274	0.135	0.058	0.810
3.25	96.77	11.56	0.290	0.144	0.060	0.770
3.00	83.80	10.75	0.297	0.155	0.060	0.730
2.75	75.00	10.15	0.332	0.164	0.060	0.690
2.50	63.42	9.05	0.377	0.184	0.070	0.620
2.25	54.05	8.29	0.415	0.200	0.073	0.560
2.00	45.45	7.41	0.451	0.225	0.075	0.500
1.75	36.58	6.51	0.513	0.256	0.080	0.440
1.50	29.70	5.63	0.594	0.296	0.085	0.370

TABLE A.3.19

DATA FOR ANTISHOCK POLYSTYRENE-n-HEXANE SYSTEM AT 382.3 K

<u>P</u> (kg/cm ²)	<u>Q</u> (ml/min)	<u>u</u> (cm/sec)	<u>t_R</u> (min)	<u>t_A</u> (min)	<u>w_{1/2}</u> (cm)	<u>H</u> (cm)
3.00	88.23	11.17	0.233	0.149	0.055	1.000
2.75	75.00	10.42	0.259	0.160	0.060	0.970
2.50	67.41	9.48	0.292	0.176	0.065	0.890
2.25	57.14	8.55	0.307	0.195	0.065	0.800
2.00	48.00	7.75	0.338	0.215	0.068	0.730
1.75	39.73	6.78	0.387	0.246	0.074	0.650
1.50	32.61	5.99	0.443	0.279	0.081	0.600

TABLE A.3.20

DATA FOR ANTISHOCK POLYSTYRENE-n-HEXANE SYSTEM AT 394.1 K

<u>P</u> (kg/cm ²)	<u>Q</u> (ml/min)	<u>u</u> (cm/sec)	<u>t_R</u> (min)	<u>t_A</u> (min)	<u>w_{1/2}</u> (cm)	<u>H</u> (cm)
3.50	115.38	12.35	0.207	0.135	0.035	0.520
3.00	90.91	10.81	0.235	0.154	0.035	0.400
2.75	77.92	10.10	0.255	0.165	0.035	0.340
2.50	65.93	9.13	0.280	0.182	0.035	0.280
2.25	55.55	8.33	0.302	0.200	0.035	0.240
2.00	47.62	7.66	0.340	0.217	0.035	0.190

TABLE A.3.21

DATA FOR ANTISHOCK POLYSTYRENE-n-HEXANE SYSTEM AT 402.3 K

<u>P</u> (kg/cm ²)	<u>Q</u> (ml/min)	<u>u</u> (cm/sec)	<u>t_R</u> (min)	<u>t_A</u> (min)	<u>w_{1/2}</u> (cm)	<u>H</u> (cm)
3.50	109.09	12.34	0.199	0.135	0.035	0.560
3.25	96.77	11.56	0.217	0.144	0.035	0.470
3.00	83.80	10.75	0.234	0.155	0.035	0.400
2.75	75.00	10.15	0.242	0.164	0.035	0.370
2.50	63.42	9.05	0.268	0.184	0.035	0.310
2.25	54.05	8.29	0.291	0.200	0.035	0.260
2.00	45.45	7.41	0.332	0.225	0.035	0.200
1.75	36.58	6.51	0.377	0.256	0.035	0.150
1.50	29.70	5.63	0.433	0.296	0.035	0.110

TABLE A.3.22

DATA OBTAINED FOR ANTISHOCK POLYSTYRENE-n-HEXANE

SYSTEM AT VARIOUS TEMPERATURES

P_i (mm Hg)	P_o (mm Hg)	t_R (min)	t_A (min)	Q (ml/min)	T_{col} (K)	T_{room} (K)	V_g^o (mlg ⁻¹)	V_g^{o+} (mlg ⁻¹)
1118.8	753	2.740	0.697	10.71	313.2	292.2	42.69	46.96
1302.6		1.630	0.480	17.32			35.04	
1486.5		1.180	0.373	32.14			32.14	
1671.4		0.865	0.293	34.28			28.56	
1124.8	757	2.140	0.710	11.19	325.2	289.2	31.58	33.43
1492.5		1.080	0.377	25.86			29.33	
1674.4		0.850	0.308	34.68			27.75	
1119.8	752	1.890	0.719	10.05	333.1	291.2	20.10	24.74
1303.6		1.310	0.494	15.79			20.72	
1487.5		0.950	0.383	22.81			22.70	
1671.4		0.750	0.307	31.05			23.07	

† Extrapolated to zero flow rate

TABLE A.3.22
(cont'd)

P_i (mm Hg)	P_o (mm Hg)	t_R (min)	t_A (min)	Q (ml/min)	T_{CO_2} (K)	T_{room} (K)	V_g^o (ml g ⁻¹)	$V_g^{o\ddagger}$ (ml g ⁻¹)
1120.3	752.5	1.610	0.750	10.90	343.3	289.2	17.35	18.50
1304.1		1.040	0.490	16.99			16.61	
1488.0		0.795	0.380	24.00			16.04	
1671.9		0.640	0.320	31.58			14.87	
1120.3	752.5	1.420	0.740	9.99	353.1	289.2	13.39	13.92
1304.1		1.050	0.520	15.38			12.97	
1488.0		0.700	0.390	23.07			11.52	
1120.3	752.5	1.320	0.720	10.00	363.2	290.2	11.61	12.48
1304.1		0.895	0.500	15.38			10.88	
1488.1		0.690	0.398	22.14			10.38	
1671.9		0.565	0.330	28.57			9.85	
1120.3	752.5	1.500	0.816	8.33	373.3	290.2	11.19	11.73
1304.1		0.915	0.528	14.70			10.06	
1488.0		0.690	0.408	20.83			9.76	
1671.9		0.540	0.320	28.57			9.22	

TABLE A.3.22
(cont'd)

P_i (mm Hg)	P_o (mm Hg)	t_R (min)	t_A (min)	Q (ml/min)	T_{col} (K)	T_{room} (K)	V^o (mlg ⁻¹)	$V^o \dagger$ (mlg ⁻¹)
1304.1	752.5	0.858	0.522	14.35	382.3	290.2	8.53	9.37
1488.0		0.155	0.410	20.13			7.92	
1671.9		0.525	0.333	27.27			7.68	
1303.6	752.0	0.806	0.542	13.76	394.1	291.2	6.41	6.81
1487.5		0.632	0.425	19.23			6.37	
1671.4		0.500	0.340	26.09			6.09	
1303.6	752.0	0.780	0.540	12.00	402.3	291.2	5.18	5.47
1487.5		0.620	0.450	18.50			5.03	
1671.4		0.490	0.352	24.19			4.88	

TABLE A.3.23

DATA OBTAINED FOR SBR-BENZENE SYSTEM

AT VARIOUS TEMPERATURES

P_i (mm Hg)	P_o (mm Hg)	t_R (min)	t_A (min)	Q (ml/min)	T_{col} (K)	T_{room} (K)	V_g^o (mlg ⁻¹)	$V_g^{o \dagger}$ (mlg ⁻¹)
1303.1	751.5	2.930	0.370	21.20	343.3	299.2	96.15	95.94
1488.5		2.190	0.280	31.30			96.12	
1668.9		1.750	0.220	42.86			96.32	
1303.1	751.5	2.250	0.342	20.72	353.3	298.2	70.26	74.43
1488.5		1.730	0.283	29.41			68.65	
1668.9		1.360	0.227	40.00			66.50	
1303.1	751.5	2.100	0.360	20.13	358.3	298.2	62.26	63.92
1488.5		1.500	0.276	30.61			60.54	
1668.9		1.230	0.223	40.54			60.34	
1121.7	754	2.900	0.560	11.41	363.1	293.2	53.60	55.00
1305.6		1.870	0.380	19.04			51.36	
1489.5		1.420	0.290	27.39			50.78	

† Extrapolated to zero flow rate

TABLE A.3.24

DATA OBTAINED FOR SBR CYCLOHEXANE SYSTEM

AT VARIOUS TEMPERATURES

P_i (mm Hg)	P_o (mm Hg)	t_R (min)	t_A (min)	Q (ml/min)	T_{col} (K)	T_{room} (K)	V_g^o (mlg ⁻¹)	$V_g^{o \dagger}$ (mlg ⁻¹)
1303.1	751.5	1.930	0.370	21.20	343.3	299.2	58.31	58.06
1488.5		1.440	0.280	31.30			58.38	
1688.9		1.150	0.220	42.86			58.55	
1303.1	751.5	1.500	0.340	20.72	353.3	298.2	42.72	43.60
1488.5		1.170	0.280	29.41			42.23	
1668.9		0.940	0.230	40.00			41.85	
1303.1	751.5	1.390	0.358	20.13	358.3	298.2	37.00	37.94
1488.5		1.010	0.276	30.61			36.24	
1668.9		0.825	0.223	40.54			35.95	
1121.7	754.0	2.000	0.560	11.41	363.1	293.2	32.99	32.57
1305.6		1.340	0.380	19.04			33.09	
1673.4		0.820	0.230	38.22			33.80	

† Extrapolated to zero flow rate

TABLE A.3.25

DATA OBTAINED FOR SBR-n-HEXANE SYSTEM

AT VARIOUS TEMPERATURES

P_i (mm Hg)	P_o (mm Hg)	t_R (min)	t_A (min)	Q (ml/min)	T_{col} (K)	T_{room} (K)	V_g^o (ml g ⁻¹)	$V_g^{o \dagger}$ (ml g ⁻¹)
1303.1	751.5	1.060	0.370	21.20	343.3	299.2	25.91	26.46
1488.5		0.780	0.280	31.30			25.16	
1688.9		0.620	0.220	42.86			25.18	
1303.1	751.5	0.860	0.340	20.72	353.3	298.2	19.15	19.98
1488.5		0.670	0.280	29.41			18.50	
1688.9		0.540	0.230	40.00			18.27	
1303.1	751.5	0.815	0.358	20.13	358.3	298.2	16.35	16.35
1488.5		0.607	0.276	30.61			16.34	
1688.9		0.497	0.223	40.54			16.36	
1117.2	749.5	1.150	0.550	12.00	363.1	294.2	14.41	14.41
1301.1		0.800	0.380	19.05			14.41	
1485.0		0.620	0.290	27.00			14.59	

† Extrapolated to zero flow rate

TABLE A.3.26

DATA OBTAINED FOR PIB-BENZENE SYSTEM

AT VARIOUS TEMPERATURES

P_i (mm Hg)	P_o (mm Hg)	t_R (min)	t_A (min)	Q (ml/min)	T_{col} (K)	T_{room} (K)	V_g^o (mlg ⁻¹)	$V_g^{o \dagger}$ (mlg ⁻¹)
1685.8	767.0	2.420	0.200	52.63	313.1	286.2	195.83	191.18
1502.5		2.900	0.250	40.00			194.35	
1318.6		3.890	0.310	26.78			193.53	
1134.7		5.770	0.460	16.22			192.62	
1659.3	740.5	1.820	0.200	50.80	323.1	292.7	132.84	131.40
1476.0		2.250	0.260	37.60			132.28	
1292.1		2.950	0.320	25.75			132.18	

† Extrapolated to zero flow rate

TABLE A.3.27

DATA OBTAINED FOR PIB-CYCLOHEXANE SYSTEM

AT VARIOUS TEMPERATURES

P_i (mm Hg)	P_o (mm Hg)	t_R (min)	t_A (min)	Q (ml/min)	T_{col} (K)	T_{room} (K)	V_g^o (ml g ⁻¹)	$V_g^{o \dagger}$ (ml g ⁻¹)
1502.5	767.0	3.280	0.250	40.00	313.1	287.2	221.43	229.48
1318.6		4.400	0.320	27.27			223.72	
1134.7		6.520	0.480	16.80			226.18	
1685.5	767.0	2.030	0.200	52.63	323.1	287.2	160.87	157.97
1502.5		2.550	0.250	38.00			159.67	
1318.6		3.270	0.320	26.90			159.56	

† Extrapolated to zero flow rate

TABLE A.3.28

DATA OBTAINED FOR PIB-n-PENTANE SYSTEM

, AT VARIOUS TEMPERATURES

P_i (mm Hg)	P_o (mm Hg)	t_R (min)	t_A (min)	Q (ml/min)	T_{col} (K)	T_{room} (K)	v_g^o (ml g ⁻¹)	$v_g^{o \dagger}$ (ml g ⁻¹)
1134.7	767.0	1.500	0.470	16.80	313.1	287.2	38.56	39.04
1318.6		1.010	0.320	27.27			37.85	
1502.5		0.770	0.240	39.00			37.76	
1134.7	767.0	1.240	0.460	16.22	323.1	287.2	28.19	29.19
1318.6		0.830	0.320	27.27			27.97	
1502.5		0.640	0.250	38.00			27.00	

† Extrapolated to zero flow rate

APPENDIX 4

REQUIRED PHYSICAL PROPERTIES OF SOLVENTS

A.4.1. Calculation of Saturated Vapor Pressures of Pure Solvents (P_1^S)

The Antoine equation was used to estimate the pure component vapor pressures :

$$\ln P_1^S = A - B/(T + C) \quad (\text{A.4.1})$$

A,B,C are constants, obtained from references (31).

A.4.2. Estimation of Molar Liquid Volume of Solvents (V_1)

The equation for calculating reduced density (ρ_r) is given as (39):

$$\rho_r = 1.20 + (5.563 - 11.03 z_c) (1 - T_r)^{(0.8z_c + 0.31)} \quad (\text{A.4.2})$$

where z_c is the compressibility factor and can be obtained by :

$$z_c = \frac{P_c V_c}{R T_c} \quad (\text{A.4.3})$$

The molar volume of pure solvent is calculated from :

$$V_1 = \frac{V_c}{\rho_r} \quad (\text{A.4.4})$$

A.4.3. Second Virial Coefficient (B_{11})

B_{11} values were obtained from references (40).

APPENDIX 5

SAMPLE CALCULATIONS

Sample calculations for n-hexane solvent and 10 % antishock polystyrene loading at the column temperature of 402.3 K.

A.5.1. V_g^0 :

Linear regression method was used to extrapolate specific retention volumes to zero flow rates.

Q (ml/min)	V_g^0 (mlg ⁻¹)
12.00	5.18
18.50	5.03
24.19	4.88

Extrapolated Value of $V_g^0 = 5.47 \text{ mlg}^{-1}$
(see Table A.3.22)

A.5.2. Ω_1^∞ :

$$M_1 = 8617 \text{ ggmole}^{-1}$$

$$B_{11} = - 845 \text{ ccmmole}^{-1}$$

$$V_g^0 = 5.47 \text{ mlg}^{-1}$$

$$V_1 = 154.64 \text{ ccmmole}^{-1}$$

$$P_1^s = 4.91 \text{ atm}$$

$$T = 402.3 \text{ K}$$

By equation (3.6) :

$$\ln \Omega_1^\infty = \ln \left[\frac{(273.2)(82.05)}{(4.91)(5.47)(86.17)} \right] = \frac{4.91}{(-82.05)(402.3)} (-845 - 154.64)$$

$$\Omega_1^\infty = 11.26 \text{ (See Table 5.3)}$$

A.5.3. χ :

$$P_1^S = 4.91 \text{ atm}$$

$$M_n = 73486$$

$$V_g^O = 5.47 \text{ ml g}^{-1}$$

$$V_1 = 154.64 \text{ cc mole}^{-1}$$

$$M_1 = 86.17 \text{ gg mole}^{-1}$$

$$B_{11} = -845$$

$$V_{2sp} = \frac{1}{0.915 \text{ g/cc}} = 1.093 \text{ cc g}^{-1}$$

By Eq. (3.14)

$$\chi = \ln \frac{(273.2)(82.05)(1.093)}{(5.47)(4.91)(154.64)} - \left[1 - \frac{154.64}{(73486)(1.093)} \right] - \frac{(4.91)}{(82.05)(402.3)} (-845 - 154.64)$$

$$\chi = 0.93 \text{ (see Table 5.3)}$$

A.5.4. D_1 :

By Eq. (3.21), H is calculated from the known values of $w_{1/2}$ and t_R (see Table A.3.21). Using H versus u values, the slope of the curve was found to be $C = 0.060$.

By using Eq. (3.24) :

$$\rho_p = 0.915 \text{ gcc}^{-3}$$

$$R = 8.15 \times 10^{-3} \text{ cm}$$

$$\delta = 0.11$$

$$\rho_B = 0.47 \text{ gcc}^{-3}$$

$$d_f = \frac{(0.11/0.915)}{\{3/(8.15 \times 10^{-3})(0.47)\}} = 0.15 \times 10^{-3} \text{ cm}$$

By using Eq. (3.20)

$$C = 0.060$$

$$d_f = 0.15 \times 10^{-3} \text{ cm}$$

$$k = 0.4$$

$$0.060 = \frac{8}{\pi^2} \frac{(0.15 \times 10^{-3})^2}{D_1} \frac{0.4}{(0.4 + 1)^2}$$

$$D_1 = 6.2 \times 10^{-8} \text{ cm sec}^{-2} \quad (\text{see Table 5.6})$$

A.5.5. ΔH_s :

By Eq. (3.17) :

<u>Data points</u>		<u>1/T</u>
$T_1 = 382.3 \text{ K}$	→	26.15×10^{-4}
$T_2 = 390.4 \text{ K}$	→	25.15×10^{-4}
$T_3 = 394.1 \text{ K}$	→	25.37×10^{-4}
$T_4 = 402.3 \text{ K}$	→	24.80×10^{-4}
$V_{g1}^0 = 0.37 \text{ ml g}^{-1}$	→	$\ln V_{g1}^0 = 2.24$
$V_{g2}^0 = 7.70 \text{ ml g}^{-1}$	→	$\ln V_{g2}^0 = 2.04$
$V_{g3}^0 = 6.81 \text{ ml g}^{-1}$	→	$\ln V_{g3}^0 = 1.92$
$V_{g4}^0 = 5.47 \text{ ml g}^{-1}$	→	$\ln V_{g4}^0 = 1.69$
$R = 1.987 \text{ cal gmole}^{-1}$		

Using $\ln V_g^0$ versus $1/T$ values, the slope of the curve was found to be 4219.1 by regression method.

$$-\frac{\Delta H_s}{R} = 4219.1 ; -\Delta H_s = (4219.1)(1.987) = 8383 \text{ cal gmole}^{-1}$$

$$-\Delta H_s = 8.4 \text{ kcal gmole}^{-1} \quad (\text{see Table 5.8})$$